



# GIS-based forest fire susceptibility modeling in Pauri Garhwal, India: a comparative assessment of frequency ratio, analytic hierarchy process and fuzzy modeling techniques

Anuj Tiwari<sup>1</sup> · Mohammad Shoab<sup>2</sup> · Abhilasha Dixit<sup>3</sup>

Received: 4 May 2020 / Accepted: 26 September 2020 / Published online: 14 October 2020  
© Springer Nature B.V. 2020

## Abstract

This study performs a comparative evaluation of Frequency Ratio (FR), Analytic Hierarchy Process (AHP), and Fuzzy AHP (FAHP) modeling techniques for forest fire susceptibility mapping in Pauri Garhwal, Uttarakhand, India. Locations of past forest fire events reported from November 2002 to July 2019 were collected from the Uttarakhand Forest Department and Forest Survey of India and combined with the ground observations obtained from the manual survey. Then, the locations were categorized into two groups of 70% (10,500 locations) and 30% (4500 locations), randomly, for training and validation purposes, respectively. Forest fire susceptibility mapping was performed on the basis of fourteen different topographic, biological, human-induced and climatic criteria such as Digital Elevation Model, Slope, Aspect, Curvature, Normalized Difference Vegetation Index, Normalized Difference Moisture Index, Topographic Wetness Index, Soil, Distance to Settlement, Distance to Road, Distance to Drainage, Rainfall, Temperature, and Wind Speed. The Receiver Operating Characteristic curve and the Area Under the Curve (AUC) were implemented for validation of the three achieved Forest Fire Susceptibility Maps. The AUC plot evaluation revealed that FAHP has a maximum prediction accuracy of 83.47%, followed by AHP (81.75%) and FR (77.21%). Thus, the map produced by FAHP exhibits the most satisfactory properties. Results and findings of this study will help in developing more efficient fire management strategies in both the open and the protected forest areas (Rajaji and Jim Corbett National Park) of the district.

**Keywords** Forest fire susceptibility map (FFSM) · Multi-criteria decision analysis (MCDA) · Frequency ratio (FR) · Analytical hierarchical process (AHP) · Fuzzy analytical hierarchical process (FAHP)

---

✉ Anuj Tiwari  
atiwari2@ce.iitr.ac.in

Extended author information available on the last page of the article

## 1 Introduction

According to the recent reports of global Forest Resources Assessment (FRA) of the Food and Agriculture Organization (FAO), United Nations, world forests occupy an area of 4.06 billion hectares, representing 30.60% of the planet's total surface area (Fao 2015). Forests are the primary natural resources and nature's most enormous bounty to humanity that play a central role in sustaining ecological balance and shaping the journey of human civilization. But forests around the world are under threat, jeopardizing all the advantages. The threats manifest themselves in the form of deforestation and forest degradation. Along with other factors, forest fires are the significant cause of deforestation and forest degradation (Hosonuma et al. 2012). The increasing rate of forest fires directly causing a steep reduction in biodiversity, deforestation, and climate change, across the world. The significance of the damage caused by forest fires vary in different regions since fire intensity depends on local topographical patterns and climatic conditions (Jazireie 2005). India is one of the ten most forest-rich countries in the world. According to the latest India State of Forest Report (ISFR) by Forest Survey of India (FSI), the total forest cover of India is estimated as 802,100 km<sup>2</sup>, which constitutes 24.39% of the country's geographical area (Jadhav et al. 2019). The recent years have witnessed an alarming rise in forest fires across India. According to the Real-Time Forest Alert System of FSI, the number of forest fires increased to 14,107 from 4225 between November 2018 and February 2019 (Elavarasan et al. 2019). These cases of forest fires occur regularly in many parts of India. In 12 months, approximately 20,000 occurrences of forest fires are stated in Indian forests, particularly from the states having the most rugged topography. These states are Himachal Pradesh, Jammu and Kashmir, Manipur, Nagaland, Tamil Nadu, and Uttarakhand (Sahana and Ganaie 2017). Amongst all these hilly states, Uttarakhand stands out as having the most forest fires in highly rugged topography (AVHRR and VIRSAA 2016).

The northern state of India, Uttarakhand is mostly forested (24,240 km<sup>2</sup>, 45.32% of the state's geographical area) and consistently displays forest fire activity from February to June, with a peak in fire events in May and June (AVHRR and VIRSAA 2016). Every year, forest fires in different districts of Uttarakhand (Uttarkashi, Dehradun, Rudraprayag, Tehri, and Pauri Garhwal) cause significant loss to the forest ecosystem, diversity of flora and fauna and economic wealth. Pauri Garhwal district is home to one of the last remaining stretches of dense forests in Uttarakhand. Chir pine (*Pinus roxburghii*), deodar (*Cedrus deodara*), and blue pine (*Pinus wallichiana*) trees of the district are very susceptible to fires (Negi and Kumar 2016). According to Global Forest Watch, in May 2018, this district witnessed the highest number of fires among all districts in the country (Hughes 2018). The uncontrolled forest fires not only kill thousands of smaller mammals, ground-nesting birds, insects, and reptiles but also cause severe long-term effects by destroying habitats and food sources in the protected forest range of the Rajaji and the Jim Corbett National Park of the district. To minimize the devastating impact of forest fires and to maintain healthy forest reserves, solutions must be developed using state of the art space technology. These solutions will help the disaster response units and administrations to prepare for forest fire risk assessment, management, and prevention.

Efforts to study the factors governing forest fire spread and other measures of fire behavior were started with the development of different theoretical (Wallace 1946; van Wagner 1967; Albin 1985), semi-empirical (Frandsen 1971; Catchpole et al. 1998; Vega et al. 1998) and empirical models (Cheney et al. 1998; Hargrove et al. 2000). These models were based on the series of equations that correlate different climatic attributes to the fire

behavior indicators and provide the most elementary notions of forest fire dynamics. Later, in Mediterranean Europe, the United States, Canada, and Australia, to develop completely operational models which could forecast all types of forest fire behaviors, these equations are integrated to develop different forest fire computational systems (like McArthur fire-danger Grasslands and Forest Meters) (Noble et al. 1980). The gradual introduction of computers as work tools in the 1980s prompted the appearance of forest fire operational models, which were based on different mathematical concepts. Since then, several researchers developed and tested different operational models such as Behave (Burgan 1984), Csiro fire calculator (Crane 1982), FARSITE (Finney 1998), FBP System (Taylor and Alexander 1966), FireLab (Guarnieri et al. 1998) to predict fire behaviors and identify fire risk zones. These computationally enriched probabilistic models started allowing operators to utilize the Geographic Information System (GIS) layers. The adaptation of GIS helped forest fire researchers to make a qualitative leap forward, which was primarily needed for forest fire risk assessment and future planning (Blanchi et al. 2002). In contrast to probabilistic techniques, statistical techniques are more appropriate for modeling forest fires when the study area is large (Cumming 2001). This is because statistical techniques can receive and execute the geospatial dataset of a vast area with diverse scales and resolutions. Various statistical techniques were developed and implemented for forest fire modeling, such as logistic regression (Vasconcelos et al. 2001), Monte Carlo simulations (Gardner et al. 1999), and multiple linear regression (Chuvieco and Salas 1996; Cruz et al. 2002). In the last one decade, large number of researchers have implemented machine learning and deep learning techniques like support vector machines (Zammit et al. 2006; Petropoulos et al. 2010), random forest (Oliveira et al. 2012), maximum entropy (Liu and Yang 2013), deep convolutional neural network (Zhang et al. 2016), and artificial neural network (Zhang et al. 2009; Satir et al. 2016) for mapping and modeling different forest fire indicators. Nowadays, GIS, in integration with Remote Sensing technology, is increasingly employed in all the different perspectives of forest fire prediction, prevention and management (Sahana and Ganaie 2017; Chuvieco and Salas 1996; Chuvieco and Congalton 1989; Ambrosia et al. 1998; Keane et al. 2001; Jaiswal et al. 2002; Erten et al. 2004; Dong et al. 2005; Pradhan et al. 2007; Chavan et al. 2012; Adab et al. 2013; Pourghasemi 2016; Ljubomir et al. 2019).

Frequency Ratio (FR) is an easy to implement statistical forest fire susceptibility mapping technique. The FR has a key advantage that it is able to analyze the historical link between forest fire causative criteria and the distribution of past forest fire locations as well as determine whether a given range of causative criteria values will be threatening in the case of forest fire occurrences or not (Sahana and Ganaie 2017; Pradhan et al. 2007). Statistical modeling technique-based FFSMs are prone to uncertainties due to size and distribution of available training dataset (Sahana and Ganaie 2017; Pradhan et al. 2007; Chavan et al. 2012). Multi-Criteria Decision Analysis (MCDA) techniques have been developed to make decisions in situations where decision-making criteria are conflicting, and the selection between alternatives is complex (Greco et al. 2016). The most popular and commonly used MCDA technique is the AHP. AHP is a heuristic-based flexible, robust, and simple MCDA approach which uses the crisp numerical values of intrinsic data elements for the evaluation of criteria (Bouyssou et al. 2006). It disintegrates the problem into a hierarchy and guarantees that both qualitative and quantitative perspectives are integrated into the investigation. Since AHP addresses the issue of the subjectivity inherent in individual evaluations, it is recognized as an improvement compared to other statistical decision-making techniques. However, AHP has its own limitations. The crisp numerical values cannot consider the complexity and the uncertainty associated with the judgment of decision makers.

The decision difficulty of forest fire risk analysis is normally under ambiguity (Bouyssou et al. 2006; Chandio et al. 2013). Thus, conventional AHP technique might not enough to provide effective decision in forest fire susceptibility mapping. As fuzziness is a natural component of decision-making problems, the FAHP technique has been developed to address this issue by enabling decision makers to define approximate preferences through fuzzy numbers (Kahraman et al. 2003). This gives a much better and more exact representation of the relationship between criteria and alternatives.

The aim of the current study is to perform a comparative assessment of GIS and Remote Sensing enabled FR, AHP and FAHP techniques for forest fire susceptibility mapping. Satellite images, topographic maps, meteorological datasets and different auxiliary information collected from diversified sources are used with selected techniques to produce FFSMs in the Pauri Garhwal district of Uttarakhand, India. This study is one of the few detailed research works conducted for identification and mapping of forest fire susceptibility zones in one of the most adversely affected districts of Pauri Garhwal in Uttarakhand, India. The main difference between this study and the approaches described in the aforementioned researches is that we have implemented FAHP technique and compared the results with AHP and FR techniques in the selected study area. Also, a diversified set of expert viewpoints are utilized for determining the rules and conditioning criteria weights in AHP and FAHP. Fourteen causative criteria helped to thoroughly investigate the possible influences of every possible forest fire precondition and activity with reference to topographical, biological, anthropogenic and climatic characteristics of selected study area. Therefore, it is predicted to have better results than the past studies.

## 2 Material and methods

### 2.1 Study area

The study area of this research is the Pauri Garhwal district of Uttarakhand state of India. Location map of the study area is shown in Fig. 1. The geographic location extent of Pauri Garhwal district lies in between 78°24' E to 79°23' E Longitude and 29°45' N to 30°15' N Latitude. Being situated at the foothills of the Garhwal Himalaya, this region comprises of dense forest areas, tall grassland, shrub land and cultivated farmlands, thus ideally providing enough forest fuel and favorable conditions for forest fires. This district has total geographic area of 5329 km<sup>2</sup>, out of which the major area of total 3269 km<sup>2</sup> is under forest cover. Total forest area is divided into three major forest divisions, namely Garhwal forest division (Garhwal Circle), Lansdowne forest division (Shivalik Circle) and Corbett tiger reserve (under control of Director Corbett tiger reserve) (Tyagi and Veer 2016). Together these three divisions hold 519 km<sup>2</sup> of very dense forest, 1954 km<sup>2</sup> of moderately dense forest and 796 km<sup>2</sup> open forest cover. The protected forest range of Rajaji and Jim Corbett National Park provide a safe home for native plants and animals. A major part of Jim Corbett National Park (912.67 km<sup>2</sup>) and Rajaji National Park (249.80 km<sup>2</sup>) fall in Pauri Garhwal district. This district is also enriched with different tree species. Reverie forests present in areas of lower elevations. Different varieties of bamboos found in patches or mixed with the main species. The altitudinal variation of Chir pine forests are found from 900 to 1500 m. Oak forests present at altitude ranging from 800 m to the highest elevations. Deodar forests are confined to areas of maximum elevation (Gaur and Bartwal 1993; Dobhal 2005; Sharma et al. 2010). In the last ten years, in terms of forest fire incidents, among all

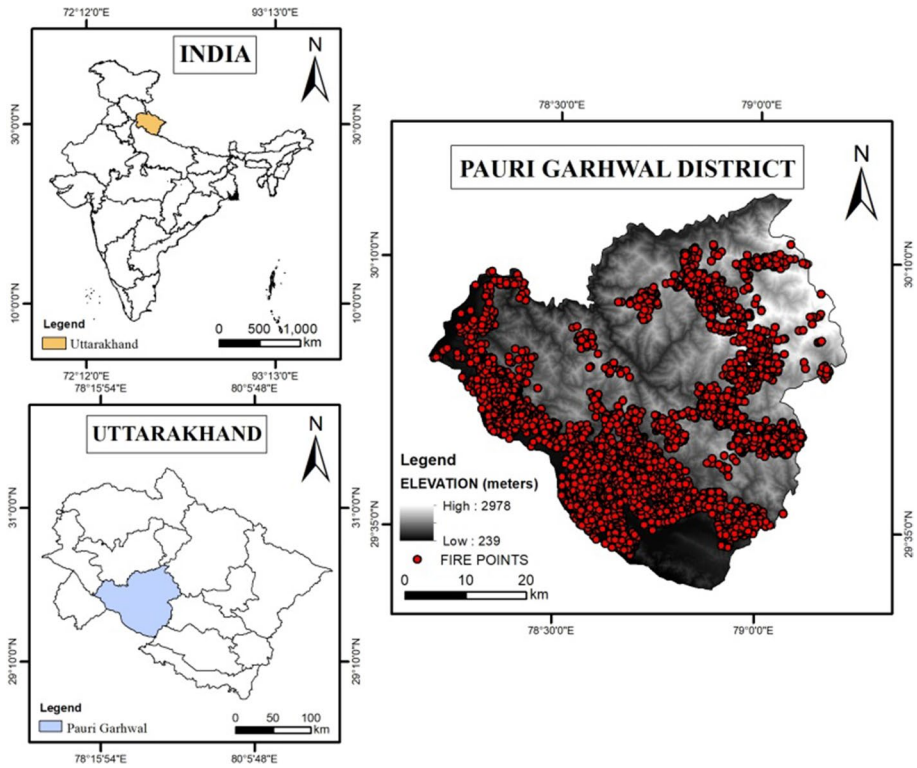


**Fig. 1** Location map of the study area with past forest fire locations (November 2002–July 2019)

the districts of Uttarakhand, maximum incidents were reported in Pauri Garhwal (Negi and Kumar 2016). Besides, natural and accidental reasons, human intentional activities, are the prominent reason of the forest fires in Pauri Garhwal (Pandey and Ghosh 2018).

## 2.2 Data used

The collection and preparation of forest fire causative criteria was an elemental and an indispensable step for forest fire susceptibility mapping. Single satellite image from Landsat-8 satellite of Oct 21, 2019 and four elevation images of the Shuttle Radar Topography Mission (SRTM) satellite of Sep 23, 2014 were obtained from United States Geological Survey (USGS) earth explorer web portal for the selected study area. Details of Landsat-8 satellite image and SRTM DEM images are presented in Table 1. These satellite images together with other vector and raster data products were used for carrying out the current study. Details of data model and sources of different criteria maps are presented in Table 2. Maps for elevation, slope, aspect, curvature and TWI (Topographic Wetness Index) were developed from SRTM DEM. NDMI (Normalized Difference Moisture Index), and NDVI (Normalized Difference Vegetation Index) layers were developed from the Landsat-8 satellite image. Distance to settlement, distance to road and distance to drainage network were developed from digital topographical maps from Survey of India (SOI) and Quick bird images (Google Earth). Soil data was collected from the National Bureau of Soil

**Table 1** Specifications of satellite datasets

Satellite	ID	Sensor	Acquisition date	Resolution
Landsat-8	LC08_L1TP_146039_20191021_20191030_01_T1	OLI	21-Oct-2019	30 m
SRTM	SRTM1N29E078V3, SRTM1N29E079V3, SRTM1N30E078V3, SRTM1N30E079V3	NA	23-Sep-2014	30 m

**Table 2** Details of data models and sources of different criteria layers

No	Layer	Data Model	Sources
1	DEM	Raster	SRTM DEM, (USGS)
2	Slope	Raster	
3	Aspect	Raster	
4	Curvature	Raster	
5	TWI	Raster	
6	Distance to settlement	Vector (Polygon)	Toposheet, Survey of India and Google Earth
7	Distance to road	Vector (Polyline)	
8	Distance to drainage	Vector (Polyline)	
9	Soil	Vector (Polygon)	National Bureau of Soil Survey and Land Use Planning, India (NBSS-LUP)
10	NDVI	Raster	Landsat-8 OLI (USGS)
11	NDMI	Raster	
12	Rainfall	Tabular (Attribute)	Indian Meteorological Department (IMD)
13	Temperature	Tabular (Attribute)	
14	Wind speed	Tabular (Attribute)	

Survey and Land Use Planning (NBSS-LUP). Climate data (Rainfall, temperature, and wind speed) was acquired from Indian Meteorological Department (IMD). All raster datasets were scaled to 30 m spatial resolution.

### 2.3 Forest fire location points

The acquisition of forest fire incidents into a spatial inventory is requisite for forest fire susceptibility mapping and validation. Forest fire points were utilized in conducting the FR analysis and model (FR, AHP and FAHP) validations. In March 2019, a field survey was conducted in Satpuli, Pauri, Lansdowne, Rajaji and Jim Corbett National Park to access the rich forest diversity and forest fire incident locations in the study area. Figure 2 presents different field photographs depicting rich forest cover of Pauri Garhwal and different forest fire locations from March 2019, May 2018 and April 2016 forest fire events. Forest fire incidents photographs were collected from local residents and Uttarakhand Forest Department, India. Different forest beats of Rajaji and Jim Corbett National Park were visited and field photographs were taken at forest fire locations. These all locations were digitized and combined with the forest fire dataset (November 2002–July 2019), acquired from the



**Fig. 2** Field survey **a** photographs from **b** Satpuli, **c** Pauri and **d** Lansdowne town of Pauri Garhwal district depicting [e–g] rich forest covers and different forest fire incidents: [h–k] March 2019, [l–n] May 2018 and [o–r] April 2016 (Source Local Residents, Field Survey, and Uttarakhand Forest Department, India)

Uttarakhand Forest Department and Forest Survey of India (FSI) to prepare the forest fire training and validation point datasets (AVHRR and VIRSAA 2016). Out of total 15,000 forest fire points, 70% of the total forest fire points (10,500) were randomly selected and implemented as a training set in the FR technique to generate the FFSM of the study area. Figure 3a presents forest fire training point map. The remaining well distributed 30% of the total forest fire points (4500) were utilized to validate the FFSMs developed with FR, AHP and FAHP techniques. Figure 3b depicts forest fire validation point map.

### 2.4 Preparation of thematic layers using remote sensing and GIS

The SRTM satellite provides 30 m DEM images, which enable the ability to map forest topography through different quantitative terrain descriptors. As presented in Table 1,

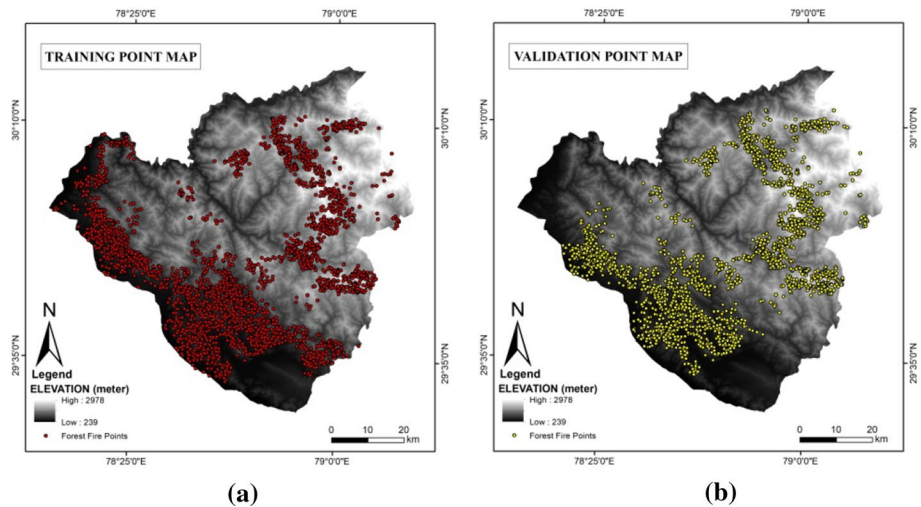


**Fig. 3** Forest fire locations (a). Training point map (used only in FR) and (b). Validation point map (used in FR, AHP and FAHP)

four SRTM DEM images covering entire study area were downloaded from USGS earth explorer web portal. These images were first mosaicked and then masked to extract DEM map of Pauri Garhwal. The DEM was projected to UTM projection with zone 43 and the horizontal and vertical datum was considered as World Geodetic System 1984 (WGS 84). The undulated terrain of Pauri Garhwal was classified into six elevation classes with 500 m altitude interval. The slope map was developed from extracted DEM image. Slope function inside ArcGIS Spatial Analyst module was used for the development of slope map. As the study area has undulated topography, resultant slope was divided into four different slope zone. An aspect map represents the direction and steepness of a continuous terrain. This map is valuable for recognizing landscape characteristics such as hills and valleys, measuring the quantity of solar illumination for surfaces, and predicting fire risks and fire compliance. Aspect map was developed by using the Aspect function in ArcGIS Spatial Analyst module. This map was classified into nine aspect classes (Flat, North, Northeast, East, Southeast, South, Southwest, West and Northwest). Curvature of a surface depicts convergence and divergence of a slope. It influences the acceleration and the deceleration of flow across the terrain and often used to determine soil erosion as well as the spread of water over the terrain. Curvature map was developed by using Curvature function in ArcGIS 3D Analyst module. It was classified into three classes such as Convex, Flat and Concave. TWI measures topographic controls of basic hydrological processes (Schillaci et al. 2015). As presented in the Eq. 1, TWI is a function of both the slope and the upstream contributing area.

$$TWI = \ln[CA/Slope] \quad (1)$$

where CA defines the local upslope catchment area and Slope represents the steepest outward slope for each grid cell (Tarboton 1997). Equation 1 was implemented with ArcGIS model builder.



Landsat-8 satellite image was first stacked and then masked with the shape file of the study area. Extracted image was used for vegetation cover and moisture extraction using NDVI and NDMI indices, respectively. NDVI determines vegetation by computing the normalized separation between the Near-Infrared (which tree/crop well reflect) and the Red light (which tree/crop well absorb) using Eq. 2. NDMI quantifies vegetation water content by computing the normalized separation between the Short-Wave-Infrared (which tree/crop water well reflect) and the Near-Infrared (which tree/crop well absorb) using Eq. 3. Histogram analysis and ground validations were used to determine threshold values for their classification. Vegetation cover extraction and moisture estimation are the essential and most widely used parameters for satellite-driven forest fire susceptibility mapping (Werf et al. 2010). Developed green forest classification was validated with India State of Forest Report by Forest Survey of India (Jadhav et al. 2019).

$$\text{NDVI} = \frac{(\text{NIR} - \text{Red})}{(\text{NIR} + \text{Red})} \quad (2)$$

$$\text{NDMI} = \frac{(\text{SWIR} - \text{NIR})}{(\text{SWIR} + \text{NIR})} \quad (3)$$

where NIR defines the Near Infrared Band and SWIR defines the Short-Wave Infrared Band. As NDVI and NDMI are normalized indices they range in between  $-1$  to  $+1$ .

Distance to settlement and distance to road were prepared from Quick bird images (Google Earth) and digital topographical maps from Survey of India (SOI). Digital topographical maps were scanned, rectified and digitized to develop settlements and roads. For more detailed mapping, settlements and roads were also extracted from Google Earth images. Together, these two datasets provided detailed thematic maps for settlements and roads. The drainage map was prepared with the Survey of India topographical map by first scanning it, then rectifying and digitizing it using ArcGIS software. Distance to settlement, distance to road and distance to drainage network maps were developed using Euclidean distance function in ArcGIS Spatial Analyst module. The soil map of the study area was collected from the National Bureau of Soil Survey and Land Use Planning, India (NBSS-LUP).

The rainfall, temperature and wind speed datasets for Bironkhol, Landsdown, Pauri and Srinagar IMD Station over 20 years (1998–2018) time period were procured from Indian Meteorological Department (IMD). The annual average rainfall, temperature and wind speed distribution maps were prepared using nonlinear Inverse Distance-Weighted (IDW) spatial interpolation technique. IDW estimates the value at an unobserved location considering the values of neighboring observed points, which are computed inversely by their distance to the points (Wu et al. 2010; Ruelland et al. 2008).

## 2.5 Frequency ratio

When evaluating the probability of an event within a certain time interval and within a specific spatial extent, it is of major significance to determine the conditions that can cause the event and the process that could trigger the event. Mathematically, FR defines the probability of occurrence of an attribute. If we construct an incident E, and certain attributes attributed to F, the FR probability of F can be described with Eq. 4 (Pradhan et al. 2007; Sahoo et al. 2017):

$$P(E/F) = P(E \cap F)/P(F) \quad (4)$$

FR is frequently and effectively used in different applications like landslide risk zonation, flood hazard mapping, forest fire susceptibility analysis, groundwater potential delineation, etc. (Senici et al. 2010; Rahmati et al. 2016; Al-Abadi 2017; Hong et al. 2017). This technique is a popular choice for forest fire susceptibility mapping using different geospatial datasets (Pradhan et al. 2007; Sahoo et al. 2017; Senici et al. 2010; Pourtaghi et al. 2015). To compute the FR for each class of the causative criteria, an interrelationship has been established between the forest fire inventory map and criteria map using Eq. 5.

$$FR = \frac{A/B}{M/N} \quad (5)$$

where  $A$  defines the number of forest fire pixels for each class of each causative criterion;  $B$  defines the total number of pixels with forest fire events;  $M$  symbolizes the number of pixels for each class of the parameter; and  $N$  defines total number of pixels. FR values specify the proportional association to forest fire occurrence. The greater the value, the higher the probability of forest fire, and the lower the value, lowers the risk of forest fire. The calculated FR value is summed to develop a Forest Fire Susceptibility Map (FFSM) using Eq. 6.

$$FFSI = FR_1 + FR_2 + \dots + FR_n \quad (6)$$

where FFSI represents forest fire susceptibility index and  $n$  symbolizes the number of selected causative criteria. FFSI is reclassified to develop FFSM.

## 2.6 Analytic hierarchy process (AHP)

AHP is one of the most extensively implemented MCDA techniques for forest fire risk zonation and susceptibility analysis (Chavan et al. 2012; Stipanicev et al. 2007; Mahdavi 2012; Thakur and Singh 2014; Chhetri and Kayastha 2015; Eskandari 2017). In this study, AHP is utilized to examine the thematic layers representing causative criteria and to generate the FFSM using ESRI ArcGIS software. Topographic, biological, human, and climatic criteria are identified and organized in a hierarchy concerning the aim of the current research work. The next step is to compute the relative weightage for individual criterion, considering that all the criteria have different superiority and sensitivity in forest fire generation. Relative weights are assigned to individual criterion and their sub-classes from prior knowledge of criteria characteristics, local field experience, personal observation, particularities of the decided study area and expert's suggestions. The members of the group of experts are selected from Indian Institute of Technology-Roorkee, India, Indian Institute of Remote Sensing-ISRO, Dehradun, India, and Uttarakhand Forest Department, India. After the assignment of relative ranks to individual criterion using Table 3, pair-wise comparisons are made between all possible pairs of the forest fire causative criteria, and the results of these comparisons are used to develop a pair-wise comparison matrix. Now, values of all criteria are normalized by the eigenvalue–eigenvector method, and the resultant normalized pair-wise matrix is analyzed for consistency (Saaty 1980). After achieving the consistency of criteria, the coefficients of the significance (weights) are determined. Mathematical descriptions of different steps are summarized in the following points:

**Table 3** Saaty’s scale for pair-wise comparisons (Saaty 1980)

Intensity of importance	Definition	Explanation
1	Equally important	Two elements contribute equally to the objective
3	Moderately important	Decision slightly support one element over another
5	Strongly important	Decision strongly support one element over another
7	Very strongly important	One element is supported very strongly over another
9	Extremely important	Highest possible order for supporting one element over another
2,4,6,8	Intermediate values	When compromise is required
Reciprocals	Opposites	Used for inverse comparison

1. Principal eigenvalue ( $\lambda_{max}$ ) is calculated with eigenvector using Eq. 7 (Kanga et al. 2017):

$$\lambda_{max} = \frac{1}{n} \sum_{Wt_i=1}^n \frac{(CV)_i}{Wt_i} \tag{7}$$

where  $Wt$  represents the corresponding eigenvector of  $\lambda_{max}$ ,  $Wt_i$  defines weight for ranking,  $CV$  represents the consistency vector and  $n$  symbolizes total number of classes.  $CV$  is computed by multiplying pair-wise comparison matrix with the weight matrix as presented in Eq. 8.  $\lambda$  is computed by dividing the elements of  $CV$  by corresponding weights. Average of these values is represented by  $\lambda_{max}$ .

$$CV = a_{ij} \times Wt_i \tag{8}$$

$$CV = \begin{bmatrix} a_{11} & a_{12} & a_{13} & \dots & a_{1n} \\ a_{21} & a_{22} & a_{23} & \dots & a_{2n} \\ \dots & \dots & \dots & \dots & \dots \\ \dots & \dots & \dots & \dots & \dots \\ a_{n1} & a_{n2} & a_{n3} & \dots & a_{nn} \end{bmatrix} \times \begin{bmatrix} Wt_1 \\ Wt_2 \\ \dots \\ \dots \\ Wt_n \end{bmatrix}$$

where  $a_{ij}$  defines pair-wise comparison matrix in which  $a_{ii} = 1$  and  $a_{ij} = 1/a_{ji}$ .  $Wt_i$  defines the weight value for ranking. Values of  $i$  and  $j$  ranges from 1 to  $n$  (number of criteria).

2. Consistency Index (CI) represents the degree of consistency and calculated with Eq. 9 (Saaty 1980). Consistency Ratio (CR) defines the final consistency of weights assigned to causative criteria (Eq. 10) (Kanga et al. 2017; Kayet et al. 2018).

$$CI = \frac{(\lambda_{max} - n)}{(n - 1)} \tag{9}$$

$$CR = \frac{CI}{RI} \tag{10}$$

where  $n$  is the number of classes.  $CR$  should be less than 0.10 for consistent weights (Barzilai 1998). Random Index (RI) value is referred from Table 4.

**Table 4** Random index (RI) for different number of criteria (n)

<i>n</i>	1	2	3	4	5	6	7	8	9	10	11	12	13	14
RI	0	0	0.58	0.90	1.12	1.24	1.32	1.41	1.45	1.49	1.51	1.54	1.56	1.57

3. FFSI is calculated by integrating all the causative criteria of forest fires using weighted linear combination equation presented in Eq. 11 (Kanga et al. 2017; Kayet et al. 2018):

$$\text{FFSI} = \sum_{t=1}^m \sum_{f=1}^n (\text{NW}_t * C_f) \quad (11)$$

where  $\text{NW}_t$  symbolizes the normalized weight,  $C_f$  represents the rank value,  $m$  defines number of criteria and  $n$  defines the number of classes.

## 2.7 Fuzzy set theory and fuzzy membership function

In 1965, Zadeh proposed the concept of fuzzy logic to manage ambiguity and uncertainty in the input data elements (Zadeh 1965). The critical principle of fuzzy logic is that the fuzzy system members are described with fuzzy membership functions. In 2010, Zimmerman described the fuzzy set theory as presented in the Eq. 12 (Zimmermann 2010). Let  $X$  is a set of elements expressed generically by  $x$ , then a fuzzy set  $\tilde{A}$  in  $X$  is a set of ordered pairs:

$$\tilde{A} = \{x, \mu_{\tilde{A}}(x)|x\} \quad (12)$$

where  $\mu_{\tilde{A}}(x)$  defines membership function, computed with Eq. 13, which maps elements to the membership space,

$$\mu_{\tilde{A}}(x) : X \rightarrow [0, 1] \quad (13)$$

where  $X$  defines the universal set for a specific problem and  $\mu_{\tilde{A}}(x)$  refers to grade of membership for element  $x$  in fuzzy set  $A$  (Zadeh 1965; Jiang and Eastman 2000; Wood and Dragicvic 2007).

To develop a fuzzy logic-based model, the suitable membership function and its parameters must be correctly decided. As per the nature of causative criteria and the defined objective, liner (monotonically increasing or monotonically decreasing), sigmoidal (monotonically increasing or symmetric) and discrete categorical data membership functions were implemented in the current study. The fuzzy membership function tool in ESRI ArcGIS software was used to derive membership functions.

## 2.8 Fuzzy AHP

FAHP is a technique of incorporating vagueness or fuzziness of human thoughts in decision making (Kahraman et al. 2003). In the current study, we implemented Triangular Fuzzy Numbers (TFNs) to extend the crisp numerical definition of criteria for forest fire susceptibility mapping (Vahidnia et al. 2008). The membership function  $\mu_A(x)$  presented

**Fig. 4** Triangular fuzzy number representation

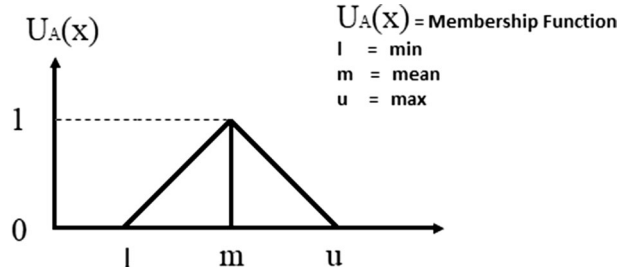


**Table 5** Triangular fuzzy numbers (TFNs) of linguistic variables for pair-wise comparisons

Linguistic variables	TFNs	Reciprocal TFNs
Extreme strongly	(9,9,9)	(1/9,1/9,1/9)
Very strongly	(6,7,8)	(1/8,1/7,1/6)
Strong	(4,5,6)	(1/6,1/5,1/4)
Moderately strong	(2,3,4)	(1/4,1/3,1/2)
Equally strong	(1,1,1)	(1,1,1)
Intermediate	(7,8,9), (5,6,7), (3,4,5), (1,2,3)	(1/9,1/8,1/7), (1/7,1/6,1/5), (1/5,1/4,1/3), (1/3,1/2,1/1)

in Fig. 4 and described in Eq. 14, defines the level of association of an element  $x$  in the domain  $X$  using the fuzzy number  $A$ .

$$\mu_A(x) = \begin{cases} \frac{x-l}{m-l}, & l \leq x \leq m \\ \frac{u-x}{u-m}, & m \leq x \leq u \\ 0, & \text{otherwise} \end{cases} \tag{14}$$

where  $l$ ,  $m$ , and  $u$  represent the lower, mean and upper bounds of the TFN, respectively.

Many FAHP techniques have been proposed in literature (Wang et al. 2008; Tiryaki and Ahlatcioglu 2009). Current study deploys Buckley fuzzy extent analysis (Buckley 1985), which is easier to compute than other FAHP techniques. Buckley’s fuzzy extent analysis has following five steps:

1. Considering the opinion of different experts, the pair-wise triangular fuzzy comparison matrix (Eq. 15) is formed.

$$\tilde{A}^k = a_{ij}^k = \begin{bmatrix} a_{11}^k & a_{12}^k & \dots & \dots & a_{1n}^k \\ a_{21}^k & a_{22}^k & \dots & \dots & a_{2n}^k \\ \dots & \dots & \dots & \dots & \dots \\ \dots & \dots & \dots & \dots & \dots \\ a_{n1}^k & a_{n2}^k & \dots & \dots & a_{nn}^k \end{bmatrix} \tag{15}$$

where  $\tilde{A}$  defines the pair-wise comparison matrix and  $a_{ij}^k$  symbolizes the expert’s choice of  $i$ th attribute over  $j$ th attribute.  $a_{ij} = (l_{ij}, m_{ij}, u_{ij})$  and  $a_{ij}^{-1} = (\frac{1}{u_{ji}}, \frac{1}{m_{ji}}, \frac{1}{l_{ji}})$  for  $i, j = 1, \dots, n$  and  $i \neq j$  using Table 5.

- As more than one experts are consulted, preferences of each expert  $a_{ij}$  are averaged and mean value  $\check{d}_{ij}$  is computed with Eq. 16. The updated matrix ( $\check{A}$ ) is presented in Eq. 17.

$$\check{d}_{ij} = \frac{\sum_{k=1}^K a_{ij}^k}{K} \tag{16}$$

$$\check{A} = \begin{bmatrix} \check{d}_{11} & \check{d}_{12} & \dots & \dots & \check{d}_{1n} \\ \check{d}_{21} & \check{d}_{22} & \dots & \dots & \check{d}_{2n} \\ \dots & \dots & \dots & \dots & \dots \\ \dots & \dots & \dots & \dots & \dots \\ \check{d}_{n1} & \check{d}_{n2} & \dots & \dots & \check{d}_{nn} \end{bmatrix} \tag{17}$$

- Next, the geometric mean of fuzzy comparison values of each criteria is computed with Eqs. 18 and used in 19 to compute the fuzzy weights.

$$\check{r}_i = \left( \prod_{j=1}^n \check{d}_{ij} \right)^{1/n}, \quad i = 1, 2 \dots n \tag{18}$$

$$\check{W}_i = \check{r}_i \otimes (\check{r}_1 \otimes \check{r}_2 \dots \otimes \check{r}_n)^{-1} = (l_i, m_i, u_i) \tag{19}$$

where  $\check{r}_i$  represents TFN and  $\check{W}_i$  represents the fuzzy weights.

- Since  $(l_i, m_i, u_i)$  are still TFNs, they require to first de-fuzzified (Chou and Chang 2008) and then normalized with Eqs. 20 and 21, respectively.

$$M_i = \frac{l_i + m_i + u_i}{3} \tag{20}$$

$$NW_i = \frac{M_i}{\sum_{i=1}^n M_i} \tag{21}$$

where  $M_i$  is a crisp and non-fuzzy number and  $NW_i$  represents normalized weights.

- Similar to Eq. 11, FFSI is calculated by multiplying each alternative weight with related criteria using Eq. 22.

$$FFSI = \sum_{t=1}^m \sum_{f=1}^n (NFW_t * FC_f) \tag{22}$$

where  $NFW_t$  represents the normalized fuzzy weight,  $FC_f$  defines the normalized score of each class,  $m$  defines the number of criteria and  $n$  defines the number of classes.

### 2.9 Validation of forest fire susceptibility maps

Validation is a critical step in forest fire susceptibility mapping which is vital for determining the predictive capability of selected modeling techniques (Mohammadi et al. 2014; Pourghasemi et al. 2016). To access the accuracy of the forest fire susceptibility mapping using FR, AHP and FAHP techniques, in the current study the AUC-ROC curve was

implemented with forest fire validation dataset. It is the standard technique most frequently employed in GIS and Remote Sensing-based susceptibility mapping studies to evaluate the modeling accuracy (Rahmati et al. 2016; Mallick et al. 2019; Shahabi et al. 2015; Park et al. 2011). The ROC depicts the trade-off between the two rates (Negnevitsky 2005) and AUC provides scale and classification-threshold-invariant way to measure the quality of the model's predictions capability (Bradley 1997).

## 3 Result

### 3.1 Thematic layers

Fourteen different criteria (DEM, Slope, Aspect, Curvature, Distance to Settlement, Distance to Road, Distance to Drainage, NDVI, NDML, TWI, Soil, Rainfall, Temperature and Wind Speed) were integrated for forest fire susceptibility mapping in the selected study area. Map presenting causative criteria are shown in Fig. 5. Criteria layers are raster, vector and tabular in nature and classified using natural break (Jenks), manual, equal interval and textural units. Table 6 summarizes criteria layer, corresponding data types and classification methods. The detailed description of individual layer is presented in the following sub-sections.

#### 3.1.1 DEM

Elevation is a critical physiographic criterion that governs fire behavior by affecting the volume and schedule of rainfall, as well as exposure to prevailing wind (Chuvieco and Congalton 1989; Buechling and Baker 2004; Gaither et al. 2011). Elevation also affects the vegetation patterns, air humidity and warmer-drier conditions of soils and fuels during the fire season (Falkowski et al. 2005). The elevation map (DEM) of the study area is divided into six elevation zones of 500 m interval, that is, (1) < 500 m, (2) 500–1000 m, (3) 1000–1500 m, (4) 1500–2000 m, (5) 2000–2500 m (6) > 2500 m (Fig. 5a). The study area is primarily occupied by lower altitude regions, followed by relatively high regions with hilly areas. The four elevation zones (up to 2000 m) occupy 92.55% of the entire region, while the next two elevation zones (of hilly region) occupy 7.45% of the study area.

#### 3.1.2 Slope

One of the critical criteria that affects the rate of fire spread is the slope degree (Viegas 2004). Fire propagation is faster in higher slope regions and less instantly in lower slope regions (Mermoz et al. 2005). The slope map is categorized into four classes such as (1) < 20°, (2) 20°–30°, (3) 30°–40°, and (4) > 40° (Fig. 5b). Pauri Garhwal is primarily owned by medium slope range, followed by relatively high slope regions. The highest slope region (> 30°) occupies 27.13% of the entire region, while the medium slope range (20°–30°) occupies 31.83% of the total area.

#### 3.1.3 Aspect

Aspect affects the amount of sunlight and temperature a site receives. As the selected study area lies inside the northern hemisphere, south-facing aspects receive maximum

**Fig. 5** Forest fire causative criteria map **a** DEM, **b** Slope, **c** Aspect, **d** Curvature, **e** Distance to settlement, **f** Distance to road, **g** Distance to drainage, **h** NDVI, **i** NDMI, **j** TWI, **k** Soil, **l** Rainfall, **m** Temperature, and **n** Wind speed

solar radiation while north-facing aspects remain coolest (Hayes 1941; Cerdà et al. 1995; Courtney Mustaphi and Pisaric 2013). Also, during the day, east aspects receive higher ultraviolet and straight sunlight in comparison to the west aspect (Beaty and Taylor 2001). Aspects also control the vegetation patterns, temperatures variations, winds flow, humidity, and fuel moistures (Pourtaghi et al. 2015; Iwan et al. 2004). The aspect map is divided into nine classes such as (1) Flat, (2) North, (3) Northeast, (4) East, (5) Southeast, (6) South, (7) Southwest, (8) West and (9) Northwest using equal interval (Fig. 5c). North aspect region occupies 36.42%, South aspect region occupies 38.42%, East aspect region occupies 34.83%, West aspect region occupies 39.22% and Flat region occupies 0.78% of the study area.

### 3.1.4 Curvature

Curvature defines the rate of change of gradient (slope) (Troeh 1965). In this way, an increase in gradient (positive) represents the convex curvature (for example, Hill), a decrease in gradient (negative) represents the concave curvature (for example Valley), and constant gradient (zero) represents the flat surface (Childs et al. 2004). Curvature governs the propagation of fire (Vakalis et al. 2004). In the current study, the curvature map is divided into three classes, such as (1) Convex, (2) Flat, and (3) Concave. As shown in Fig. 5d, 43.66% has convex terrain and 50.09% of the study area has concave terrain. While remaining 6.25% is flat.

### 3.1.5 Distance to settlement

The closeness of forest space to the rural and the urban settlements is a critical parameter for evaluating the extent of urbanization-induced anthropogenic stress and other associated problems like forest fires, deforestation, overexploitation of forest resources, etc. (Jaiswal et al. 2002; DeFries and Pandey 2010). People residing near the forest areas can, directly and indirectly, induce accidental fires (Erten et al. 2004). As different settlement patches are inhabited within the forest range of Pauri Garhwal, so it is essential to include distance to settlement as a causative criterion. The proximity of these settlements with the forest and small dwelling spacings (< 2 m) provide ample opportunity for direct flame impingement to spread the fire from forest to dwelling and dwelling to dwelling, with the combination of high fuel loads and small, reasonably ventilated enclosures resulting in speedy development times from ignition through flashover into fully developed stages (Erten et al. 2004). As a result, fires can spread into multiple dwellings extremely fast. The finite element technique and a standard fire model were generally used for determining the displacements and strains developed in structural members exposed to fire (Erten et al. 2004). As shown in Fig. 5e, distance to settlement map is divided into four classes, such as (1) < 500 m, (2) 500–1000 m (3) 1000–1500 m and (4) > 1500 m. Buffer zone of 500 m helps to find a close correlation between forest fire incidents and settlements boundaries.



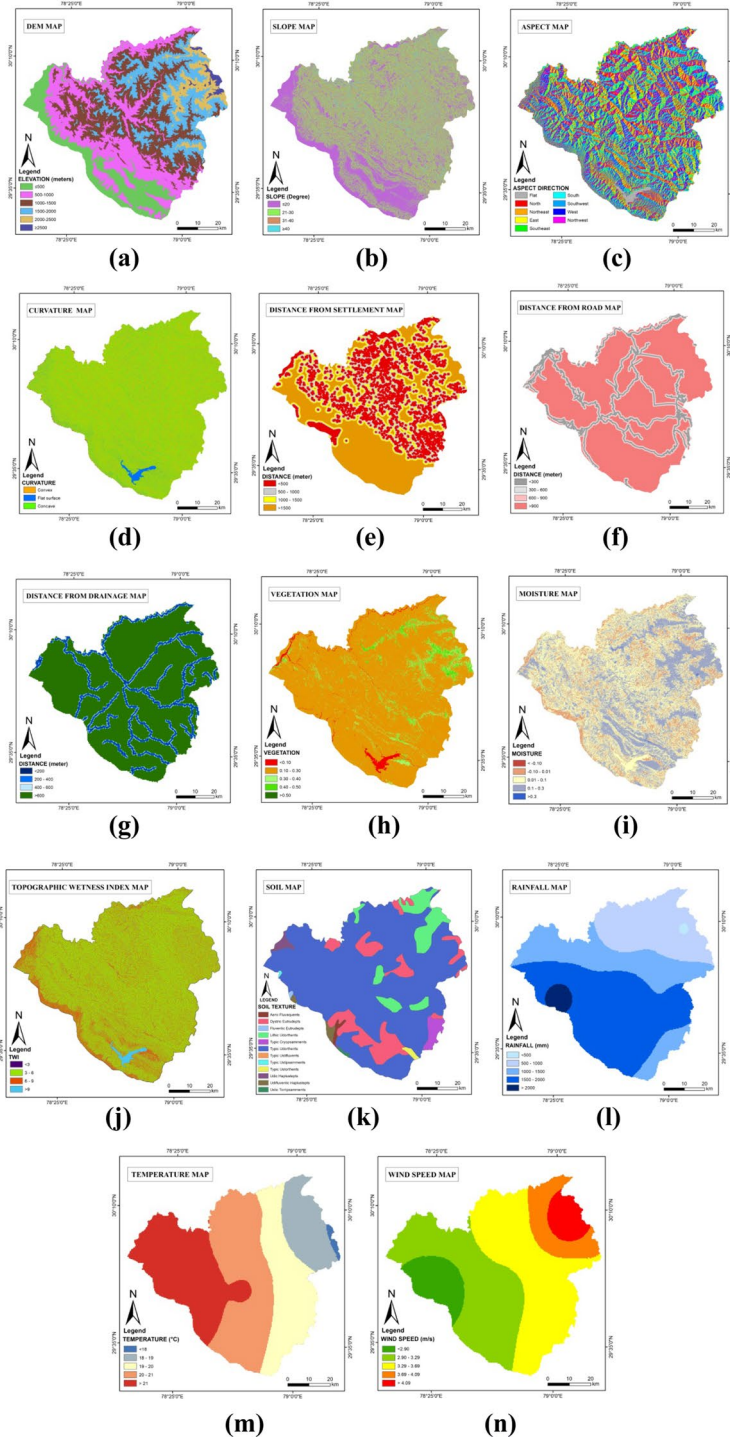


**Table 6** Causative criteria, data types and classification methods

No.	Layer	Data type	Classification method
1	DEM	Raster	Natural break
2	Slope	Raster	Natural break
3	Aspect	Raster	Equal interval-directional units
4	Curvature	Raster	Natural break
5	Distance to settlement	Vector (Polygon)	Manual
6	Distance to road	Vector (Polyline)	Manual
7	Distance to drainage	Vector (Polyline)	Manual
8	NDVI	Raster	Natural break
9	NDMI	Raster	Natural break
10	TWI	Raster	Natural break
11	Soil	Vector (Polygon)	Textural units-soil types
12	Rainfall	Tabular (Attribute)	Natural break
13	Temperature	Tabular (Attribute)	Natural break
14	Wind speed	Tabular (Attribute)	Natural break

### 3.1.6 Distance to road

Forest road network is an essential infrastructure framework of the forest landscape that plays a crucial role in the management and the development of forested areas (Arienti et al. 2010; Jain et al. 1996). However, different physical actions by man, animal, or vehicle on these transportation corridors can influence an unwanted fire. Therefore, proximity to the transportation network becomes an essential criterion in studying the susceptibility of the forest fire (Jaiswal et al. 2002; Demir 2007). As shown in Fig. 5f, distance to road network map is divided into four classes, such as (1) < 300 m, (2) 300–600 m (3) 600–900 m and (4) > 900 m. Based on the extent of the study area, spatial distribution, and structure of the underlying transportation structure, we selected a 300 m road buffer interval.

### 3.1.7 Distance to drainage

Pauri Garhwal district has an extensive drainage network of some of the perennial rivers (Dobhal 2005; Devi et al. 2015). This drainage network has a substantial influence on forest fire, as the distance from river/streams constrains impact, scope, and severity of forest fire (Sahana and Ganaie 2017; Chandra 2005). The drainage develops a buffer region that does not support the fire to expand. As shown in Fig. 5g, distance to drainage map is divided into four classes, such as (1) < 200 m, (2) 200–400 m (3) 400–600 m and (4) > 600 m.

### 3.1.8 NDVI

NDVI measures the plant photosynthetic activity, which in turn closely related to the soil water availability (Gamon et al. 1995; Pettorelli et al. 2005). By enabling the observation of vegetation health indicator in a localized range, the NDVI images can recognize vegetation cover that has potentially become forest fire fuel and presents an insight into the possible dangers of fire (Gandhi et al. 2015). The vegetation vigor and the hydric state of fuels helps to determine fire ignition probability, conditioning to some extent, and rate of spread

of fire (Heinsch and Andrews 2010). As shown in Fig. 5h, NDVI map is divided into five classes, such as (1)  $< 0.10$ , (2)  $0.10–0.30$  (3)  $0.30–0.40$  (4)  $0.40–0.50$  and (5)  $> 0.50$ .

### 3.1.9 NDMI

NDMI is susceptible to the moisture levels in crops and trees (Wang et al. 2013). NDMI helps to define crop's or forest's water stress level areas that are particularly susceptible to forest fire, while NDVI shows how much vegetation is available for burning or to use as fuel (Yebra et al. 2013). As shown in Fig. 5i, NDMI map is divided into five classes, such as (1)  $< -0.10$ , (2)  $-0.10–0.01$ , (3)  $0.01–0.1$ , (4)  $> 0.1–0.3$  and (5)  $> 0.3$ .

### 3.1.10 TWI

The topography is a first-order representation of the spatial variation of hydrological requirements (Dawes and Short 1994). It is a physical criterion that measures the topographic control on hydrological processes and defines the degree of accumulation of water (Sörensen et al. 2006). Water accumulates at any particular place within the catchment area and moves down with the slope of the terrain. Thus, TWI defines the spatial distribution of soil moisture and directly impacts the development of scenarios for forest fires (Adab et al. 2013). As shown in Fig. 5j, TWI map is divided into four classes, such as (1)  $< 3.0$ , (2)  $3.0–6.0$  (3)  $6.0–9.0$ , and (4)  $> 9.0$ .

### 3.1.11 Soil

Soil is one of the essential criteria in the description of forest fire and also indirectly influences the entire ecosystem of a specific region (Sharma et al. 2010; Gairola et al. 2012). Soils of the region have been formed either through paedogenetic processes (physical and chemical properties of rocks and minerals) or are transported soils (carried and deposited by the streams) (Jaiswal et al. 2002). A wide range of variations in soil type can be observed in the entire study region (Gairola et al. 2012). As shown in Fig. 5k, soil map is divided into twelve classes such as (1) Aeric Fluvaquents, (2) Dystric Eutrudepts, (3) Fluventic Eutrudepts, (4) Lithic Udorthents, (5) Typic Cryopsamments, (6) Typic Udorthents, (7) Typic Ustifluvents, (8) Typic Ustipsamments, (9) Typic Ustorthents, (10) Udic Haplustepts, (11) Udifluventic Haplustepts and (12) Ustic Torripsamments using textural units. The study area is primarily occupied by Typic Udorthents soil cover (74.84%), followed by Dystric Eutrudepts soil cover (11.87%) and Lithic Udorthents soil cover (8.88%).

### 3.1.12 Rainfall

Rainfall has an inverse relation with forest fires. Low rainfall increases the risk of forest fire by reducing moisture content of the fuels and making them susceptible to fires (Jain et al. 2013; Mondal and Sukumar 2016). The influence of precipitation on fire spreading is to reduce the air humidity, humidity of habitat and moisture content of the fuels (Mondal and Sukumar 2016). In zone of minimum precipitation, moisture content of the fuels is reduced, making the ignition prominent (Rawat 2003). Annual average rainfall map of Pauri Garhwal district is developed by using 1998 to 2018 rainfall data procured from the Indian Meteorological Department. As shown in Fig. 5l, rainfall map is divided into five

classes such as (1) < 1000 mm, (2) 1000–1300 mm (3) 1300–1600 mm (4) 1600–1900 mm and (5) > 1900 m.

### 3.1.13 Temperature

Temperature has a direct relation with forest fires. High temperature increases the risk of forest fire by making fuels highly susceptible to fires, mainly due to dryness (Flannigan et al. 2016). The frequency of forest fires is more from April to June (summer season) when both air and soil temperature are high. With the increase in temperature, forest fire fuel start reducing its moisture content and becomes more susceptible to ignition. Increasing temperature directly impacts the destructive nature, coverage, and frequency of forest fires (Chuvieco et al. 2004). Fires can occur at any temperature, but their frequency depends upon increasing temperature. Annual air average temperature map of Pauri Garhwal district is developed by using 1998 to 2018 air temperature data procured from the Indian Meteorological Department. As shown in Fig. 5m, temperature map is divided into five classes such as (1) < 18 °C, (2) 18–19 °C, (3) 19–20 °C, (4) 20–21 °C, and (5) > 21 °C.

### 3.1.14 Wind speed

Wind Speed boosts the amount of fresh oxygen in the existing fire, which appears in an immediate and rapid flame ignition (Karafyllidis and Thanailakis 1997; Dimri and Gunwant 2012). It also drops the degree of surface moisture, which enhances the drying of the fuel. High-speed and powerful-wind heads toward the rapid expansion of a fire cover. High wind speed in the summer period enhances the forest fire frequency (Kanga et al. 2017). Wind Speed map of Pauri Garhwal district is developed by using 1998 to 2018 wind speed data procured from the Indian Meteorological Department. As shown in Fig. 5n, wind speed map is divided into five classes such as (1) < 2.5 m/s, (2) 2.5–3 m/s, (3) 3–3.5 m/s, (4) 3.5–4 m/s, (5) > 4 m/s.

## 3.2 Forest fire susceptibility mapping

In the current study, FFSMs of Pauri Garhwal, Uttarakhand, have been developed by implementing FR, AHP and FAHP techniques along with fourteen different causative criteria. Detailed description of results obtained with individual technique are presented in the following sub-sections.

### 3.2.1 FR-FFSM

The spatial relationships that exist in between the incidence of forest fires and selected causative criteria were inferred using training dataset (10,500 points) and FR technique. Table 7 shows the frequency ratios of each influencing criteria. FFSI was computed using the linear summation of frequency ratios. FFSM was prepared by classifying the FFSI into five intervals (very high, high, moderate, low and very low) using natural break method. Figure 6 shows the FFSM of Pauri Garhwal, Uttarakhand, developed with FR technique. Absolute area statistics and percentage distribution of five different susceptibility classes are exhibited in Table 8. The FR technique shows that 19.58% of the area has very high, 34.25% of has high, 22.02% has moderate, 18.11% has low, and 6.04% has very low forest fire susceptibility.

**Table 7** Spatial relation of forest fire causative criteria and forest fire locations using FR

No.	Criteria	No. of pixel in domain	% Pixels in domain (a)	No. of forest fire pixel	% of forest fire pixel (b)	Frequency ratio value (b/a)
1	DEM (m) (C1)					
	< 500	907,071	14.96	1707	16.26	1.09
	500–1000	1,770,201	29.19	6179	58.85	2.02
	1000–1500	1,748,077	28.83	802	7.64	0.27
	1500–2000	1,186,993	19.57	1496	14.25	0.73
	2000–2500	386,330	6.37	310	2.95	0.46
	> 2500	65,277	1.08	6	0.06	0.06
2	Slope (degree) (C2)					
	< 20	2,488,541	41.04	5110	48.67	1.19
	20–30	1,930,133	31.83	3194	30.42	0.96
	30–40	1,248,458	20.59	1717	16.35	0.79
	> 40	396,817	6.54	479	4.56	0.70
3	Aspect (C3)					
	Flat	47,330	0.78	4	0.04	0.05
	North	737,113	12.16	1077	10.26	0.84
	Northeast	723,212	11.93	1299	12.37	1.04
	East	683,385	11.27	1273	12.12	1.08
	Southeast	704,987	11.63	1335	12.71	1.09
	South	789,859	13.03	1561	14.87	1.14
	Southwest	834,249	13.76	1706	16.25	1.18
	West	795,998	13.13	1258	11.98	0.91
	Northwest	747,816	12.33	987	9.4	0.76
4	Curvature (C4)					
	Convex	2,647,611	43.66	4542	43.26	0.99
	Flat	379,167	6.25	600	5.71	0.91
	Concave	3,037,171	50.09	5358	51.03	1.02
5	Distance to settlement (m) (C5)					
	< 500	2,099,181	34.62	910	8.67	0.25
	500–1000	1,283,175	21.16	1245	11.86	0.56
	1000–1500	677,620	11.17	1160	11.05	0.99
	> 1500	2,003,973	33.05	7185	68.43	2.07
6	Distance to road (m) (C6)					
	< 300	1,083,660	17.87	697	6.64	0.37
	300–600	650,984	10.74	551	5.25	0.49
	600–900	527,633	8.70	601	5.72	0.66
	> 900	3,801,672	62.69	8651	82.39	1.31
7	Distance to drainage (m) (C7)					
	< 200	288,743	4.76	361	3.44	0.72
	200–400	519,164	8.56	776	7.39	0.86
	400–600	225,805	3.72	313	2.98	0.80
	> 600	5,030,237	82.95	9050	86.19	1.04

**Table 7** (continued)

No.	Criteria	No. of pixel in domain	% Pixels in domain (a)	No. of forest fire pixel	% of forest fire pixel (b)	Frequency ratio value (b/a)
8	NDVI (C8)					
	< 0.10	108,561	1.79	53	0.5	0.28
	0.10–0.30	5,353,431	88.28	9856	93.87	1.06
	0.30–0.40	425,039	7.01	476	4.53	0.65
	0.40–0.50	174,971	2.89	115	1.1	0.38
	> 0.50	1947	0.03	0	0	0.00
9	NDMI (C9)					
	< 0.05	1837	0.03	0	0	0.00
	0.5–0.1	1,051,124	17.33	1160	11.05	0.64
	0.1–0.2	2,857,534	47.12	4722	44.97	0.95
	0.2–0.3	2,146,054	35.39	4610	43.9	1.24
	> 0.3	7400	0.12	8	0.08	0.67
10	TWI (C10)					
	< 3	975	0.02	0	0	0.00
	43,619	3,956,817	65.25	6957	66.26	1.02
	43,714	1,742,199	28.73	3041	28.96	1.01
	> 9	363,958	6	502	4.78	0.80
11	Soil (C11)					
	Aeric Fluvaquents	27,882	0.46	52	0.5	1.09
	Dystric Eutrudepts	719,653	11.87	1820	17.33	1.46
	Fluventic Eutrudepts	6152	0.1	1	0.01	0.10
	Lithic Udorthents	538,311	8.88	364	3.47	0.39
	Typic Cryopsamments	105,289	1.74	151	1.44	0.83
	Typic Udorthents	4,538,532	74.83	7849	74.75	1.00
	Typic Ustifluvents	92	0.01	0	0	0.00
	Typic Ustipsamments	4781	0.08	3	0.03	0.38
	Typic Ustorthents	23,042	0.38	164	1.56	4.11
	Udic Haplustepts	50,485	0.83	43	0.41	0.49
	Udifluventic Haplustepts	38,992	0.64	42	0.4	0.63
	Ustic Torripsamments	10,738	0.18	11	0.1	0.56
12	Rainfall (mm) (C12)					
	< 1000	21,326	0.35	0	0	0.00
	1000–1300	1,445,536	23.84	916	8.72	0.37
	1300–1600	1,689,820	27.87	2019	19.23	0.69
	1600–1900	2,748,269	45.32	7213	68.7	1.52
	> 1900	158,998	2.62	352	3.35	1.28

**Table 7** (continued)

No.	Criteria	No. of pixel in domain	% Pixels in domain (a)	No. of forest fire pixel	% of forest fire pixel (b)	Frequency ratio value (b/a)
13	Temperature (°C) (C13)					
	< 18	42,532	0.7	6	0.06	0.09
	18–19	796,785	13.14	394	3.75	0.29
	19–20	1,427,245	23.54	2587	24.64	1.05
	20–21	1,987,769	32.78	4346	41.39	1.26
	> 21	1,809,618	29.84	3167	30.16	1.01
14	Wind speed (m/s) (C14)					
	< 2.5	594,064	9.79	1317	12.54	1.28
	2.5–3.0	2,137,528	35.25	5576	53.1	1.51
	3.0–3.5	2,368,847	39.06	2994	28.51	0.73
	3.5–4.0	608,448	10.03	458	4.36	0.43
	> 4	355,062	5.85	155	1.48	0.25

**Table 8** Classification of forest fire susceptibility using FR, AHP and FAHP

Class	Forest fire susceptibility class	FR		AHP		FAHP	
		Area (Sq. km)	%	Area (Sq. km)	%	Area (Sq. km)	%
1	Very high	1043.48	19.58	1051.86	19.74	1067.32	20.03
2	High	1825.10	34.25	1853.88	34.79	2002.89	37.58
3	Moderate	1173.65	22.02	1292.08	24.25	1310.82	24.60
4	Low	965.06	18.11	788.01	14.79	582.78	10.94
5	Very low	321.74	6.04	343.20	6.44	365.20	6.85

### 3.2.2 AHP-FFSM

All selected criteria layers (DEM, Slope, Aspect, Curvature, Distance to Settlement, Distance to Road, Distance to Drainage, NDVI, NDMI, TWI, Soil, Rainfall, Temperature and Wind Speed) were integrated in AHP to delineate FFSM using ArcGIS raster calculator. According to the importance or the contribution of the criteria, pair-wise comparison matrix was developed by the experts to compute the weights for each criteria layer (Table 9). As shown in Table 10, CI and CR were calculated to validate the significance of weights. As, CR (0.054) of all pair-wise comparisons is less than 0.10 (Table 10), pair-wise comparison matrix is consistent in nature. Table 11 presents relative weights, potentiality and rating assigned to individual class and their sub-classes. After obtaining the final weights of criteria, the linear weighted combination was used to generate the final FFSM. As depicted in Fig. 7 and Table 8, the FFSM was divided into five intervals (very high, high, moderate, low and very low) using natural break method. The AHP technique shows that 19.74% of the area has very high, 34.79% has high, 24.25% has moderate, 14.79% has low, and 6.44% has very low forest fire susceptibility.

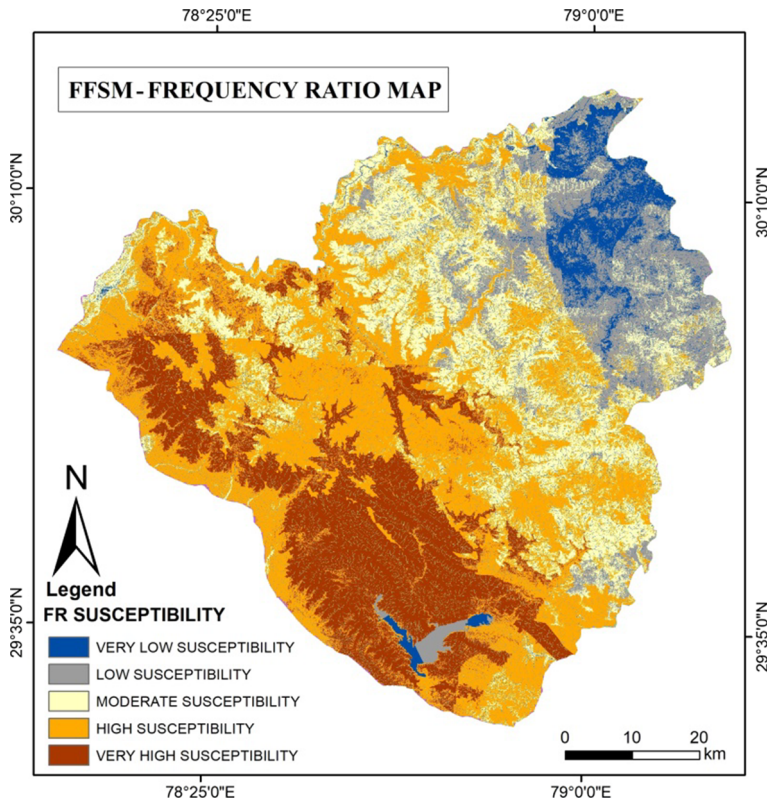


**Fig. 6** Forest fire susceptibility map using FR

**Table 9** Pair-wise comparison matrix for AHP

Criteria	C1	C2	C3	C4	C5	C6	C7	C8	C9	C10	C11	C12	C13	C14
DEM (C1)	1	1/3	4	1	2	6	6	1/4	1	8	1/2	1	1/5	2
Slope (C2)	3	1	9	6	6	9	9	2	4	9	2	3	2	9
Aspect (C3)	1/4	1/9	1	1/2	1	4	4	1/4	1/2	6	1/7	1/4	1/3	4
Curvature (C4)	1	1/6	2	1	2	9	9	1/2	1	8	1/2	2	1/2	3
Dist. to settlement (C5)	1/2	1/6	1	1/2	1	6	6	1/6	1/6	2	1/4	1/2	1/3	2
Dist. to road (C6)	1/6	1/9	1/4	1/9	1/6	1	1	1/9	1/8	1	1/8	1/5	1/6	1/2
Dist. to drainage (C7)	1/6	1/9	1/4	1/9	1/6	1	1	1/8	1/5	1	1/9	1/4	1/8	1/3
NDVI (C8)	4	1/2	4	2	6	9	8	1	2	9	1	2	1	4
NDMI (C9)	1	1/4	2	1	6	8	5	1/2	1	9	1/3	4	1/2	3
TWI (C10)	1/8	1/9	1/6	1/8	1/2	1	1	1/9	1/9	1	1/9	1/4	1/7	1/2
Soil (C11)	2	1/2	7	2	4	8	9	1	3	2	1/4	4	1	2
Rainfall (C12)	1	1/3	4	1/2	2	5	4	1/2	1/4	4	1/4	1	1	2
Temperature (C13)	5	1/2	3	2	3	6	8	1	2	7	1	1	1	4
Wind speed (C14)	1/2	1/9	1/4	1/3	1/2	2	3	1/4	1/3	2	1/2	1/2	1/4	1



**Table 10** Normalized weight matrix for AHP

Criteria	C1	C2	C3	C4	C5	C6	C7	C8	C9	C10	C11	C12	C13	C14	Weight	$\lambda$
DEM (C1)	0.05	0.08	0.11	0.06	0.06	0.08	0.08	0.03	0.06	0.12	0.07	0.05	0.02	0.05	0.07	15.42
Slope (C2)	0.15	0.23	0.24	0.35	0.17	0.12	0.12	0.26	0.26	0.13	0.28	0.15	0.23	0.24	0.21	15.63
Aspect (C3)	0.01	0.03	0.03	0.03	0.03	0.05	0.05	0.03	0.03	0.09	0.02	0.01	0.04	0.11	0.04	14.73
Curvature (C4)	0.05	0.04	0.05	0.06	0.06	0.12	0.12	0.06	0.06	0.12	0.07	0.10	0.06	0.08	0.08	14.99
Dist. to Settlement (C5)	0.03	0.04	0.03	0.03	0.03	0.08	0.08	0.02	0.01	0.03	0.04	0.03	0.04	0.05	0.04	14.65
Dist. to Road (C6)	0.01	0.03	0.01	0.01	0.00	0.01	0.01	0.01	0.01	0.01	0.02	0.01	0.02	0.01	0.01	14.41
Dist. to Drainage (C7)	0.01	0.03	0.01	0.01	0.00	0.01	0.01	0.02	0.01	0.01	0.02	0.01	0.01	0.01	0.01	14.60
NDVI (C8)	0.20	0.12	0.11	0.12	0.17	0.12	0.11	0.13	0.13	0.13	0.14	0.10	0.12	0.11	0.13	15.56
NDMI (C9)	0.05	0.06	0.05	0.06	0.17	0.11	0.07	0.06	0.06	0.13	0.05	0.20	0.06	0.08	0.09	15.53
TWI (C10)	0.01	0.03	0.00	0.01	0.01	0.01	0.01	0.01	0.01	0.01	0.02	0.01	0.02	0.01	0.01	14.54
Soil (C11)	0.10	0.12	0.18	0.12	0.12	0.11	0.12	0.13	0.19	0.03	0.04	0.20	0.12	0.05	0.12	16.28
Rainfall (C12)	0.05	0.08	0.11	0.03	0.06	0.07	0.05	0.06	0.02	0.06	0.04	0.05	0.12	0.05	0.06	15.38
Temperature (C13)	0.25	0.12	0.08	0.12	0.09	0.08	0.11	0.13	0.13	0.10	0.14	0.05	0.12	0.11	0.12	15.49
Wind Speed (C14)	0.03	0.03	0.01	0.02	0.01	0.03	0.04	0.03	0.02	0.03	0.07	0.03	0.03	0.03	0.03	14.38

Value of lambda max ( $\lambda$ ) = 15.11, Consistency index (CI) = 0.085, Consistency ratio (CR) = 0.054

**Table 11** Potentiality, rating and weight of causative criteria with corresponding sub-classes

No.	Criteria	Class	Potentiality for FFISM	Rating	Weight
1	DEM (C1)	< 500	Very high	5	0.07
		500–1000	Very high	5	
		1000–1500	Moderate	4	
		1500–2000	High	3	
		2000–2500	Low	2	
2	Slope (C2)	> 2500	Very low	1	0.21
		< 20	Low	1	
		20–30	Moderate	3	
		30–40	High	4	
		> 40	Very high	5	
3	Aspect (C3)	Flat	High	4	0.04
		North	Very low	1	
		Northeast	Low	2	
		East	Moderate	3	
		Southeast	High	4	
		South	Very high	5	
		Southwest	Very high	5	
		West	Moderate	3	
		Northwest	Low	2	
4	Curvature (C4)	Convex	Moderate	3	0.08
		Flat	Very high	5	
		Concave	High	4	
5	Dist. to Settlement (C5)	< 500	Very high	5	0.04
		500–1000	High	4	
		1000–1500	Low	2	
		> 1500	Very low	1	
6	Dist. To road (C6)	< 200	Very high	5	0.01
		200–400	High	4	
		400–600	Low	2	
		> 600	Very low	1	
7	Dist. to drainage (C7)	< 300	Very high	5	0.01
		300–600	High	4	
		600–900	Low	2	
		> 900	Very low	1	
8	NDVI (C8)	< 0.10	Very low	1	0.13
		0.10–0.30	Moderate	3	
		0.30–0.40	High	4	
		0.40–0.50	High	4	
		> 0.50	Very high	5	
9	NDMI (C9)	< 0.05	Very low	1	0.09
		0.5–0.1	Low	2	
		0.1–0.2	Moderate	3	
		0.2–0.3	High	4	
		> 0.3	Very high	5	

**Table 11** (continued)

No.	Criteria	Class	Potentiality for FFSM	Rating	Weight
10	TWI (C10)	< 3.0	Low	2	0.01
		3.0–6.0	Moderate	3	
		6.0–9.0	High	4	
		> 9.0	Very high	5	
11	Soil (C11)	Aeric Fluvaquents	Very low	1	0.12
		Dystric Eutrudepts	High	4	
		Fluventic Eutrudepts	High	4	
		Lithic Udorthents	Very high	5	
		Typic Cryosamments	Moderate	3	
		Typic Udorthents	Very high	5	
		Typic Ustifluvents	Very low	1	
		Typic Ustipsamments	Very low	1	
		Typic Ustorthents	Very low	1	
		Udic Haplustepts	Low	2	
		Udifuventic Haplustepts	Low	2	
		Ustic Torripsamments	Very low	1	
		12	Rainfall (C12)	< 1000	
1000–1300	Low			2	
1300–1600	Moderate			3	
1600–1900	High			4	
> 1900	Very high			5	
13	Temperature (C13)	< 18	Very low	1	0.12
		18–19	Low	2	
		19–20	Moderate	3	
		20–21	High	4	
		> 21	Very high	5	
14	Wind speed (C14)	< 2.5	Very low	1	0.03
		2.5–3.0	Low	2	
		3.0–3.5	Moderate	3	
		3.5–4.0	High	4	
		> 4.0	Very high	5	

### 3.2.3 FAHP-FFSM

In FAHP, all selected criteria layers were integrated to delineate FFSM using ArcGIS fuzzy membership tool and ArcGIS raster calculator. Fuzzy membership functions used for individual criteria layer with the function specific control points and resultant utility are presented in Table 12. These functions mapped an input criteria layer into the corresponding fuzzy output layer having values from 0 and 1, to indicate the degree of membership of that layer. The output fuzzy criteria layers are presented in Fig. 8. In the next step fuzzy pair-wise comparison matrix was generated with TFNs. Table 13 presents fuzzy pair-wise comparison matrix with relative fuzzy, averaged and normalized weights of fuzzy criteria layers. After obtaining the

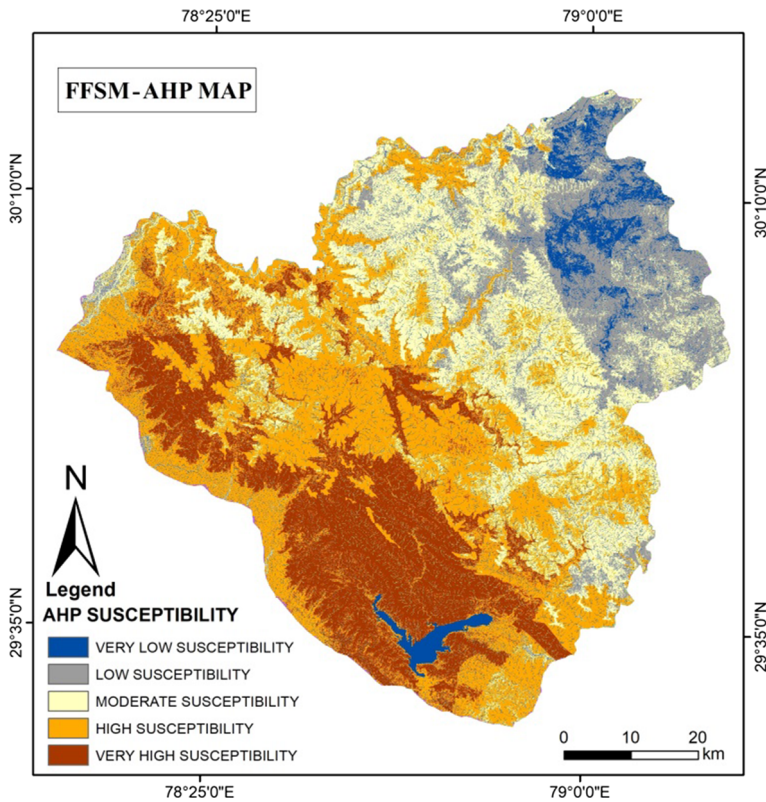


**Fig. 7** Forest fire susceptibility map using AHP

normalized weights of criteria, the linear weighted combination was used to generate the final FFSM. As shown in Fig. 9 and Table 8, the FFSM was divided into five intervals using natural break method. The FAHP technique shows that 20.03% of the area has very high, 37.58% has high, 24.60% has moderate, 10.94% has low, and 6.85% has very low forest fire susceptibility.

### 3.3 Validation

Validation of FR, AHP and FAHP techniques was performed in order to check their prediction accuracy. The ROC curves for FFSMs developed with FAHP, AHP and FR are presented in Fig. 10. The AUC plot evaluation revealed that FAHP has a maximum prediction accuracy of 83.47%, followed by AHP (81.75%) and FR (77.21%). As a result, developed FFSMs are proved to be accurate and effective for forest fire hazard preparation in the selected study area.

## 4 Discussion

Uncontrolled forest fires pose a great threat not only to the entire eco-system and bio-diversity of the forest but also to the forest wealth, human life and the local climate of the region. Considering the causes and the impacts of forest fires, it is essential to identify forest fire

**Table 12** Fuzzy membership functions, control points and final utility of causative criteria in FAHP

Criteria	Fuzzy membership function	Control points	Resultant utility
DEM (C1)	Linear monotonically decreasing	Min = 2500; Max = 1000	$<1000 = 1$ ; $1000$ to $2500 = 0$ to $1$ ; $>2500 = 0$
Slope (C2)	Linear monotonically increasing	Min = 20; Max = 40	$<20 = 0$ ; $20$ to $40 = 0$ to $1$ ; $>40 = 1$
Aspect (C3)	Sigmoidal symmetric	Min1 = 22.5; Max1 = 157.5; Min2 = 202.5; Max2 = 337.5	$337.5$ to $22.5 = 0$ ; $22.5$ to $157.5 = 0$ to $1$ ; $157.5$ to $202.5 = 1$ ; $202.5$ to $337.5 = 0$
Curvature (C4)	Sigmoidal monotonically increasing	Min = -2; Max = 1	$<-2 = 0$ ; $-2$ to $1 = 0$ to $1$ ; $>1 = 1$
Dist. to settlement (C5)	Linear monotonically decreasing	Min = 1500; Max = 500	$<500 = 1$ ; $500$ to $1500 = 0$ to $1$ ; $>1500 = 0$
Dist. to road (C6)	Linear monotonically decreasing	Min = 600; Max = 200	$<200 = 1$ ; $200$ to $600 = 0$ to $1$ ; $>600 = 0$
Dist. to drainage (C7)	Linear monotonically decreasing	Min = 900; Max = 300	$<300 = 1$ ; $300$ to $900 = 0$ to $1$ ; $>900 = 0$
NDVI (C8)	Sigmoidal monotonically increasing	Min = 0.10; Max = 0.50	$<0.10 = 0$ ; $0.10$ to $0.50 = 0$ to $1$ ; $>0.50 = 1$
NDMI (C9)	Sigmoidal monotonically increasing	Min = 0.05; Max = 0.3	$<0.05 = 0$ ; $0.05$ to $0.3 = 0$ to $1$ ; $>0.3 = 1$
TWI (C10)	Sigmoidal monotonically increasing	Min = 3.0; Max = 9.0	$<3.0 = 0$ ; $3.0$ to $9.0 = 0$ to $1$ ; $>9.0 = 1$
Soil (C11)	Discrete categorical data	Aeric Fluvaquents = 0; Ustic Torripsamments = 0; Ustic Ustorthents = 0; Typic Ustorthents = 0; Typic Ustipsamments = 0; Udic Haplustepts = 0.25; Udifluventic Haplustepts = 0.25; Typic Cryopsamments = 0.5; Dystric Entrodepts = 0.75; Fluventic Entrodepts = 0.75; Lithic Udorthents = 1; Typic Udorthents = 1	$<1000 = 0$ ; $1000$ to $1900 = 0$ to $1$ ; $>1900 = 1$
Rainfall (C12)	Linear monotonically increasing	Min = 1000; Max = 1900	$<18 = 0$ ; $18$ to $21 = 0$ to $1$ ; $>21 = 1$
Temperature (C14)	Sigmoidal monotonically increasing	Min = 18; Max = 21	$<2.5 = 0$ ; $2.5$ to $4.0 = 0$ to $1$ ; $>4.0 = 1$
Wind speed (C13)	Sigmoidal monotonically increasing	Min = 2.5; Max = 4.0	

**Fig. 8** Causative criteria, based on fuzzy membership functions, **a** DEM, **b** Slope, **c** Aspect, **d** Curvature, **e** Distance to settlement, **f** Distance to road, **g** Distance to drainage, **h** NDVI, **i** NDMI, **j** TWI, **k** Soil, **l** Rainfall, **m** Temperature and **n** Wind speed

susceptibility zones, where urbanization is growing in the close proximity of forest regions. In the current study, one statistical (FR), and two heuristic (AHP and FAHP) forest fire susceptibility mapping techniques were applied with different spatial and non-spatial causative criteria in one of the most forest enriched and bio-diversified Pauri Garhwal district of Garhwal Himalaya. Analysis of the causative criteria together with the FFSMs developed using FR, AHP and FAHP techniques help to understand the reasons and impacts of drastically increasing forest fire incidents in the region.

- The current research work presented that the most important causative criteria for forest fire identification are slope, followed by NDVI, temperature, and soil. The significance of these factors is already reported in different studies worldwide, which is consistent with the outcomes of the current study (Eskandari 2017; Pourghasemi et al. 2016; Eugenio et al. 2016; Suryabhagavan et al. 2016). Nature of the terrain (Curvature) (Alexander 1985; Weber 1989; Hilton et al. 2018) and moisture (NDMI) (Fornacca et al. 2018; Torres et al. 2018) are also found as an important causative criteria in forest fire occurrence for this region. On the other hand, in opposite to the major reason of human influence in forest fire reported by different researchers (Jaiswal et al. 2002; Erten et al. 2004; Pandey and Ghosh 2018; Bui et al. 2017), current study found that the distance to settlement and distance to road have lower impact in comparison to topographical and biological factors in the development of forest fires in the selected study area. This may be because, besides anthropogenic proximity influences, human intentional activities, especially to promote new flush of grasses, collection of minor forest produce or shifting cultivation are the prominent causes for triggering the forest fires in this region (Pandey and Ghosh 2018). There is a requirement of more specific causative criteria for defining the after human agriculture activities and human-forest interconnection.
- Forest fire susceptibility mapping described that the majority of the degraded and the deciduous forest cover from both the protected (Rajaji and Jim Corbett National Park) and the open forest zones (Birokhal, Naunidanda, Kot, Pokhara, Pabo Rikhnikh, and Yamkeshwar block from Garhwal and Lansdowne forest division) fell under high to very high fire susceptibility classes. Near about complete Rajaji national park fell inside very high susceptibility class and major area of Jim Corbett national park is under high susceptibility class. Severity of forest fire incidents in Rajaji national park and Jim Corbett national park is already reported by Porwal et al. (1997) and Sharma and Hussin (1996), respectively. Forest fire susceptibility classes presented in these studies are in consistent with the outcomes of the current study. Whereas, Dwarichal, Garhwal and Zahrikhal blocks from Garhwal and Lansdowne forest division mainly have moist forest range and falls in moderate and low fire susceptibility classes. These results are relatively similar to the results of other researchers conducted different locational studies in selected region of Pauri Garhwal (Pandey and Ghosh 2018; Saklani 2008; Kumari et al. 2017).
- Validation of the results described that, of the three mapping techniques implemented in this study, FAHP was superior to AHP and FR in successfully recognizing potential forest fire susceptibility classes. But, the performance of AHP and FR was reasonable

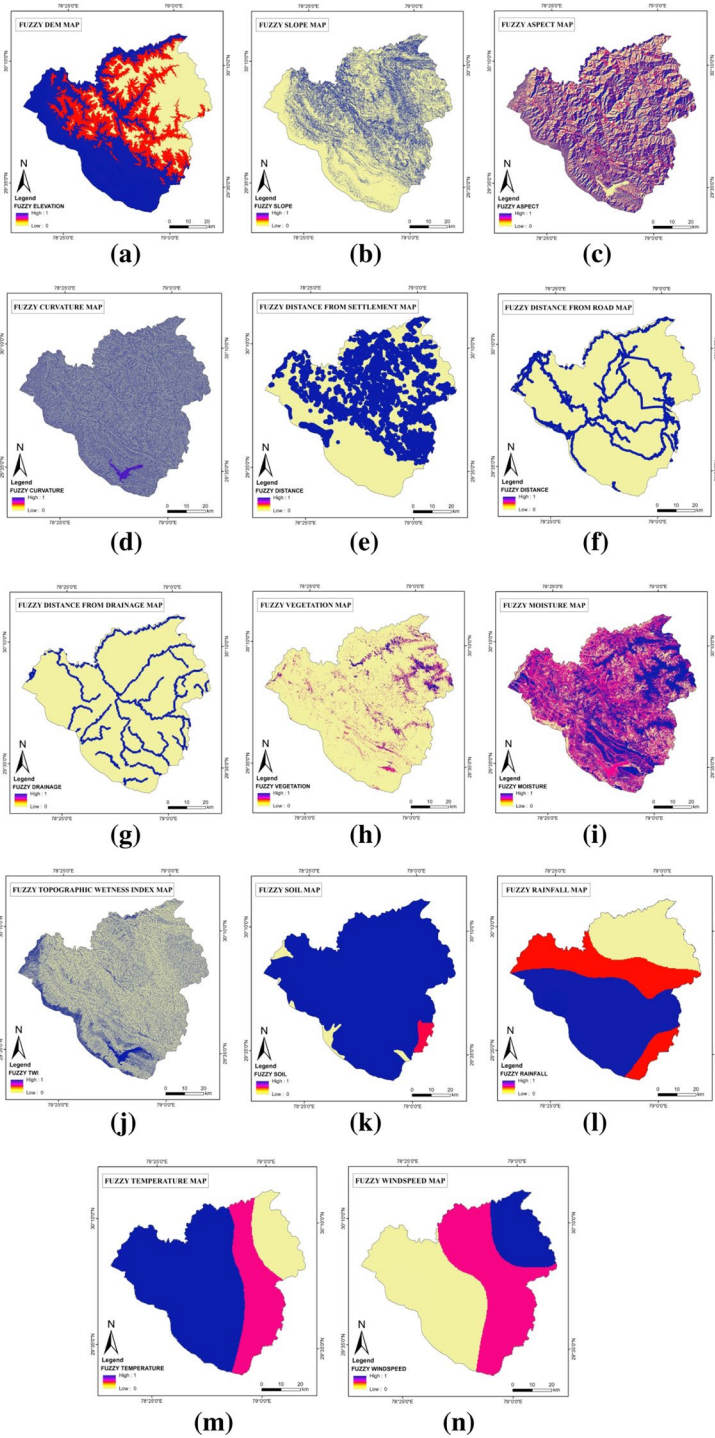


**Table 13** Pair-wise comparison matrix with relative fuzzy, averaged and normalized weights of causative criteria in FAHP (Part 1)

Criteria	C1	C2	C3	C4	C5	C6	C7	C8	C9	C10
DEM (C1)	1, 1, 1	1/4, 1/3, 1/2	3, 4, 5	1, 1, 1	1, 2, 3	5, 6, 7	5, 6, 7	1/5, 1/4, 1/3	1, 1, 1	7, 8, 9
Slope (C2)	2, 3, 4	1, 1, 1	9, 9, 9	5, 6, 7	5, 6, 7	9, 9, 9	9, 9, 9	1, 2, 3	3, 4, 5	9, 9, 9
Aspect (C3)	1/5, 1/4, 1/3	1/9, 1/9, 1/9	1, 1, 1	1/3, 1/2, 1/1	1, 1, 1	3, 4, 5	3, 4, 5	1/5, 1/4, 1/3	1/3, 1/2, 1/1	5, 6, 7
Curvature (C4)	1, 1, 1	1/7, 1/6, 1/5	1, 2, 3	1, 1, 1	1, 2, 3	9, 9, 9	9, 9, 9	1/3, 1/2, 1/1	1, 1, 1	7, 8, 9
Dist. to settlement (C5)	1/3, 1/2, 1/1	1/7, 1/6, 1/5	1, 1, 1	1/3, 1/2, 1/1	1, 1, 1	5, 6, 7	5, 6, 7	1/7, 1/6, 1/5	1/7, 1/6, 1/5	1, 2, 3
Dist. to road (C6)	1/7, 1/6, 1/5	1/9, 1/9, 1/9	1/5, 1/4, 1/3	1/9, 1/9, 1/9	1/9, 1/9, 1/9	1, 1, 1	1, 1, 1	1/9, 1/9, 1/9	1/9, 1/9, 1/9	1, 1, 1
Dist. to drainage (C7)	1/7, 1/6, 1/5	1/9, 1/9, 1/9	1/5, 1/4, 1/3	1/9, 1/9, 1/9	1/9, 1/9, 1/9	1, 1, 1	1, 1, 1	1/9, 1/8, 1/7	1/6, 1/5, 1/4	1, 1, 1
NDVI (C8)	3, 4, 5	1/3, 1/2, 1/1	3, 4, 5	1, 2, 3	5, 6, 7	9, 9, 9	7, 8, 9	1, 1, 1	1, 2, 3	9, 9, 9
NDMI (C9)	1, 1, 1	1/5, 1/4, 1/3	1, 2, 3	1, 1, 1	5, 6, 7	7, 8, 9	4, 5, 6	1/3, 1/2, 1/1	1, 1, 1	9, 9, 9
TWI (C10)	1/9, 1/8, 1/7	1/9, 1/9, 1/9	1/7, 1/6, 1/5	1/9, 1/8, 1/7	1/3, 1/2, 1/1	1, 1, 1	1, 1, 1	1/9, 1/9, 1/9	1/9, 1/9, 1/9	1, 1, 1
Soil (C11)	1, 2, 3	1/3, 1/2, 1/1	6, 7, 8	1, 2, 3	3, 4, 5	7, 8, 9	9, 9, 9	1, 1, 1	2, 3, 4	1, 2, 3
Rainfall (C12)	1, 1, 1	1/4, 1/3, 1/2	3, 4, 5	1/3, 1/2, 1/1	1, 2, 3	4, 5, 6	3, 4, 5	1/3, 1/2, 1/1	1/5, 1/4, 1/3	3, 4, 5
Temperature (C13)	4, 5, 6	1/3, 1/2, 1/1	2, 3, 4	1, 2, 3	2, 3, 4	5, 6, 7	7, 8, 9	1, 1, 1	1, 2, 3	6, 7, 8
Wind speed (C14)	1/3, 1/2, 1/1	1/9, 1/9, 1/9	1/5, 1/4, 1/3	1/4, 1/3, 1/2	1/3, 1/2, 1/1	1, 2, 3	2, 3, 4	1/5, 1/4, 1/3	1/4, 1/3, 1/2	1, 2, 3
Criteria	C11	C12	C13	C14	Relative fuzzy weights			Averaged weights		Normal-ized weights
DEM (C1)	1/3, 1/2, 1/1	1, 1, 1	1/6, 1/5, 1/4	1, 2, 3	0.0416, 0.0659, 0.1064	0.0713	0.0660			
Slope (C2)	1, 2, 3	2, 3, 4	1, 2, 3	9, 9, 9	0.1333, 0.2155, 0.3298	0.2262	0.2094			
Aspect (C3)	1/8, 1/7, 1/6	1/5, 1/4, 1/3	1/4, 1/3, 1/2	3, 4, 5	0.0232, 0.0360, 0.0604	0.0399	0.0369			
Curvature (C4)	1/3, 1/2, 1/1	1, 2, 3	1/3, 1/2, 1/1	2, 3, 4	0.0460, 0.0768, 0.1313	0.0847	0.0784			
Dist. to settlement (C5)	1/5, 1/4, 1/3	1/3, 1/2, 1/1	1/4, 1/3, 1/2	1, 2, 3	0.0214, 0.0356, 0.0634	0.0401	0.0372			
Dist. to road (C6)	1/9, 1/8, 1/7	1/6, 1/5, 1/4	1/7, 1/6, 1/5	1/3, 1/2, 1/1	0.0088, 0.0123, 0.0185	0.0132	0.0122			
Dist. to drainage (C7)	1/9, 1/9, 1/9	1/5, 1/4, 1/3	1/9, 1/8, 1/7	1/4, 1/3, 1/2	0.0089, 0.0123, 0.0182	0.0131	0.0122			
NDVI (C8)	1, 1, 1	1, 2, 3	1, 1, 1	3, 4, 5	0.0836, 0.1362, 0.2165	0.1454	0.1346			



**Table 13** (continued)

Criteria	C11	C12	C13	C14	Relative fuzzy weights	Averaged weights	Normal-ized weights
NDMI (C9)	1/4, 1/3, 1/2	3, 4, 5	1/3, 1/2, 1/1	2, 3, 4	0.0529, 0.0837, 0.1388	0.0918	0.0849
TWI (C10)	1/9, 1/9, 1/9	1/5, 1/4, 1/3	1/8, 1/7, 1/6	1/3, 1/2, 1/1	0.0090, 0.0127, 0.0193	0.0137	0.0126
Soil (C11)	1/5, 1/4, 1/3	3, 4, 5	1, 1, 1	1, 2, 3	0.0627, 0.1098, 0.1839	0.1188	0.1099
Rainfall (C12)	1/5, 1/4, 1/3	1, 1, 1	1, 1, 1	1, 2, 3	0.0348, 0.0582, 0.1006	0.0645	0.0597
Temperature (C13)	1, 1, 1	1, 1, 1	1, 1, 1	3, 4, 5	0.0723, 0.1172, 0.1868	0.1254	0.1161
Wind speed (C14)	1/3, 1/2, 1/1	1/3, 1/2, 1/1	1/5, 1/4, 1/3	1, 1, 1	0.0162, 0.0278, 0.0531	0.0324	0.0300

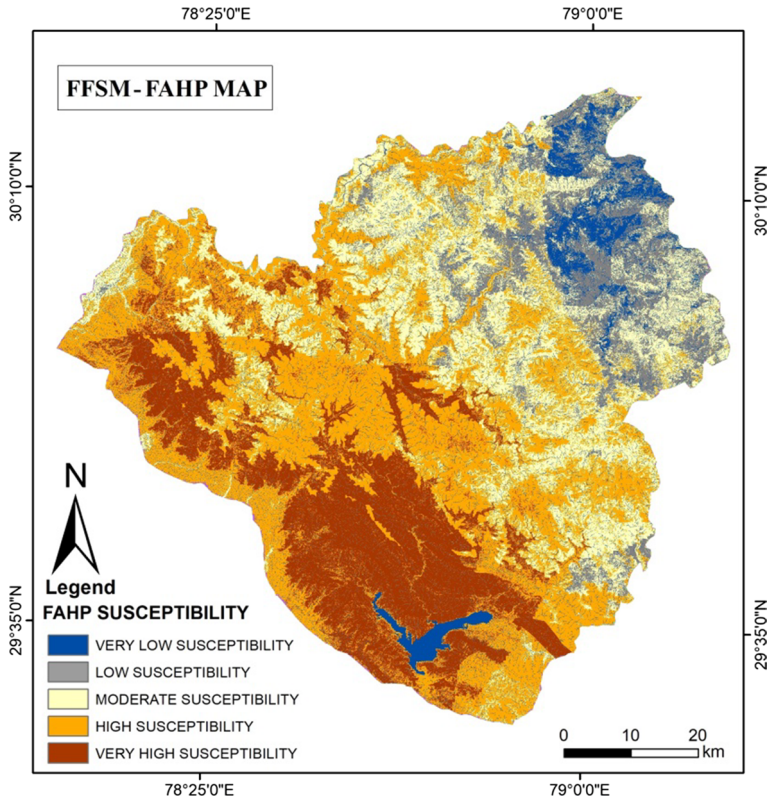


Fig. 9 Forest fire susceptibility map using FAHP

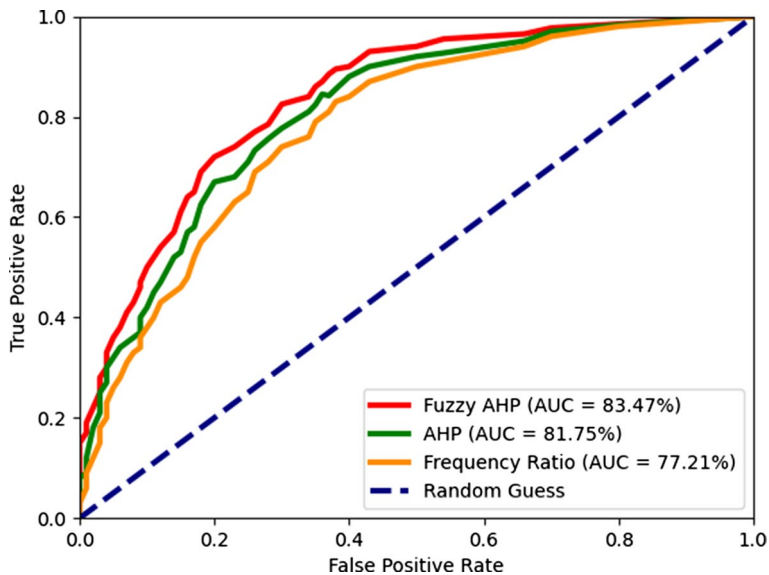


Fig. 10 ROC curves for FAHP, AHP and FR

for this study, analyzing their AUC values. The FAHP technique had a higher predictive accuracy compared with the AHP and FR techniques, which is consistent with the results of Sharma et al. (2012). Various researchers implemented different combination of FAHP, AHP and FR technique in different part of Brazil, Ethiopia, India, Iran, Turkey and Thailand (Eugenio et al. 2016; Suryabhagavan et al. 2016; Sharma et al. 2012; Hashjin et al. 2012; Akbulak et al. 2018; Nuthammachot and Stratoulis 2019; Meten et al. 2015). Their results showed that all the three techniques have the capability to produce a high-reliability FFSMs. But, in comparative assessment, the FAHP technique performed more accurately, compensating MCDM by codifying the expert knowledge for forest fire hazard and integrating it with the inherent fuzzy characteristics of the causative criteria.

The current study successfully utilizes the knowledge regarding the interrelation in between the forest fire risks and the contributions of topographic, climatic, biological and human induced causative criteria for FFSM. Although various uncertain characteristics of forest fire susceptibility require to be resolved, a level of uncertainty will always persist in any forest fire susceptibility mapping because of the uncertainty inherent in causative criteria. The uncertainty inherent lies both in the criteria weighting and in the level of importance by individual criterion. Thus, it is recommended to apply other statistical, probabilistic and machine learning techniques to develop FFSMs and compare them with the current results. This will bring more insights into how forest fire susceptibility mapping techniques select the conditioning criteria, how the forest fire phenomena are modeled under different statistical scenarios, and the reliability of the techniques.

## 5 Conclusion

Forest fires, both natural and human-induced, present a prominent threat to most of the forests and grasslands around the world. The current study demonstrated the capability of Remote Sensing and GIS techniques for developing forest fire susceptibility maps (FFSMs) in one of the most adversely affected forest fire prone districts of Pauri Garhwal, Uttarakhand, India. The study results and findings illustrated that the rich and diverse forest cover, undulated terrain, unplanned and uncontrolled urbanization, climate pattern and other features add favorable conditions to forest fire occurrence in Pauri Garhwal. The validation of the results ( $AUC > 0.5$ ) emphasizes the importance of considering a large set of causative criteria when conducting forest fire susceptibility study. This study concludes that, of the one statistical (FR), and two heuristic (AHP and FAHP) techniques, with the advantage of addressing the inherent fuzzy characteristics of the geospatial datasets and also by incorporating the subjective judgments in the modeling process, FAHP decided much more specific contributions of individual criteria layer in final forest fire susceptibility mapping. Developed FFSMs present essential information for firefighters, forest rangers, and local administrators to establish potential fire hazard zones, with the intent that they can timely and successfully perform fire prevention services. Moreover, in the protected forest range and national parks of Pauri Garhwal, FFSMs helps wildlife planners in developing fire prevention and mitigation strategies for the management of fuel material and safety of natural features and endemic species. This will also strengthen the path for developing efficient and effective land use planning, rural development, and sustainable agriculture.

In summary, the combination of thematic layers and geospatial analysis techniques implemented in this study produced an agreeable result and can be comprehensively deployed in other places for forest fire susceptibility mapping. Results are specifically conclusive in Indian perspective, where more than 36% of forest cover (657,000 km<sup>2</sup>) prone to frequent forest fires and of this, 10% highly prone and around 21% highly to extremely fire prone (FSI 2019).

**Acknowledgements** The authors would like to express their great appreciation to Dr Kamal Jain, Professor, Department of Civil Engineering, IIT Roorkee, India, for his professional guidance, enthusiastic encouragement and valuable support. The authors would also like to thank Mr. Surendra Sharma, Scientist-C, IIRS-ISRO, Dehradun, India, for his constructive suggestions during the planning and development of this research work. Our grateful thanks are also extended to Mr. Deepak Tyagi, M. Tech, NIIT University, Neemrana, Rajasthan, India, Mr. Indresh Upadhyay, DFO, Uttarakhand Forest Department, India and Mr. Anurag Joshi, Forest Ranger, Uttarakhand Forest Department, India, for their help in forest fire field data collection, analysis and interpretation.

**Funding** This research received no external funding.

## Compliance with ethical standards

**Conflict of interest** The authors declare no conflict of interest.

## References

- Adab H, Kanniah KD, Solaimani K (2013) Modeling forest fire risk in the northeast of Iran using remote sensing and GIS techniques. *Nat Hazards* 65:1723–1743
- Akbulak C, Tatlı H, Aygün G, Sağlam B (2018) Forest fire risk analysis via integration of GIS, RS and AHP: the case of Çanakkale Turkey. *J Hum Sci* 15:2127–2143
- Al-Abadi AM (2017) Modeling of groundwater productivity in northeastern Wasit Governorate, Iraq using frequency ratio and Shannon's entropy models. *Appl Water Sci* 7:699–716
- Albini FA (1985) A model for fire spread in wildland fuels by-radiation. *Combust Sci Technol* 42:229–258
- Alexander ME (1985) Estimating the length-to-breadth ratio of elliptical forest fire patterns. In: Proceedings of the eighth conference on fire and forest meteorology, vol 29. Society of American Foresters, Bethesda, MD, pp 85–04
- Ambrosia VG, Buechel SW, Brass JA, Peterson JR, Davies RH, Kane RJ, Spain S (1998) An integration of remote sensing, GIS, and information distribution for wildfire detection and management. *Photogram Eng Remote Sens* 64:977–986
- Arienti MC, Cumming SG, Krawchuk MA, Boutin S (2010) Road network density correlated with increased lightning fire incidence in the Canadian western boreal forest. *Int J Wildland Fire* 18:970–982
- AVHRR A, VIRS11 T (2016) Monitoring of forest fires from space—ISRO's initiative for near real-time monitoring of the recent forest fires in Uttarakhand India. *Curr Sci* 110:2057
- Barzilai J (1998) Consistency measures for pairwise comparison matrices. *J Multi-Crit Decis Anal* 7:123–132
- Beatty RM, Taylor AH (2001) Spatial and temporal variation of fire regimes in a mixed conifer forest landscape, Southern Cascades, California, USA. *J Biogeogr* 28:955–966
- Blanchi R, Jappiot M, Alexandrian D (2002) Forest fire risk assessment and cartography—a methodological approach. In: Proceedings of IV international conference on forest fire research, 18–23 Nov, Luso, Portugal
- Bouyssou D, Marchant T, Pirlot M, Tsoukias A, Vincke P (2006) Evaluation and decision models with multiple criteria: stepping stones for the analyst, vol. Springer, Berlin
- Bradley AP (1997) The use of the area under the ROC curve in the evaluation of machine learning algorithms. *Pattern Recogn* 30:1145–1159
- Buckley J (1985) Fuzzy decision making with data: applications to statistics. *Fuzzy Sets Syst* 16:139–147
- Buechling A, Baker WL (2004) A fire history from tree rings in a high-elevation forest of Rocky mountain national park. *Can J For Res* 34:1259–1273

- Bui DT, Bui Q-T, Nguyen Q-P, Pradhan B, Nampak H, Trinh PT (2017) A hybrid artificial intelligence approach using GIS-based neural-fuzzy inference system and particle swarm optimization for forest fire susceptibility modeling at a tropical area. *Agric For Meteorol* 233:32–44
- Burgan RE (1984) Behave: fire behavior prediction and fuel modeling system, fuel subsystem, Inter-mountain forest and range experiment station, forest service, US, vol 167
- Catchpole W, Catchpole E, Butler B, Rothermel R, Morris G, Latham D (1998) Rate of spread of free-burning fires in woody fuels in a wind tunnel. *Combust Sci Technol* 131:1–37
- Cerdà A, Imeson A, Calvo A (1995) Fire and aspect induced differences on the erodibility and hydrology of soils at La Costera, Valencia, southeast Spain. *CATENA* 24:289–304
- Chandio IA, Matori ANB, WanYusof KB, Talpur MAH, Balogun A-L, Lawal DU (2013) GIS-based analytic hierarchy process as a multicriteria decision analysis instrument: a review. *Arab J Geosci* 6:3059–3066
- Chandra S (2005) Application of remote sensing and gis technology in forest fire risk modeling and management of forest fires: a case study in the Garhwal Himalayan Region. In: Van Oosterom P, Zlatanova S, Fendel E (eds) *Geo-information for disaster management*. Springer, Berlin, pp 1239–1254
- Chavan M, Das K, Suryawanshi R (2012) Forest fire risk zonation using remote sensing and GIS in Huynial watershed, Tehri Garhwal district, UA. *Int J Basic Appl Res* 2:6–12
- Cheney N, Gould J, Catchpole WR (1998) Prediction of fire spread in grasslands. *Int J Wildland Fire* 8:1–13
- Chhetri SK, Kayastha P (2015) Manifestation of an analytic hierarchy process (AHP) model on fire potential zonation mapping in Kathmandu Metropolitan City Nepal. *ISPRS Int J GeoInf* 4:400–417
- Childs C, Kabot G, Murad-al-shaikh M (2004) Working with ArcGIS spatial analyst. ESRI, USA
- Chou S-W, Chang Y-C (2008) The implementation factors that influence the ERP (enterprise resource planning) benefits. *Decis Support Syst* 46:149–157
- Chuvieco E, Congalton RG (1989) Application of remote sensing and geographic information systems to forest fire hazard mapping. *Remote Sens Environ* 29:147–159
- Chuvieco E, Salas J (1996) Mapping the spatial distribution of forest fire danger using GIS. *Int J Geogr Inf Sci* 10:333–345
- Chuvieco E, Cocero D, Riano D, Martin P, Martinez-Vega J, de la Riva J, Pérez F (2004) Combining NDVI and surface temperature for the estimation of live fuel moisture content in forest fire danger rating. *Remote Sens Environ* 92:322–331
- Courtney Mustaphi CJ, Pisaric MF (2013) Varying influence of climate and aspect as controls of montane forest fire regimes during the late Holocene, south-eastern British Columbia Canada. *J Biogeogr* 40:1983–1996
- Crane W (1982) Computing grassland and forest fire behaviour, relative humidity and drought index by pocket calculator. *Aust For* 45:89–97
- Cruz MG, Alexander ME, Wakimoto RH (2002) Predicting crown fire behavior to support forest fire management decision making. In: Viegas DX (ed) *Forest fire research and wildland fire safety. Proceedings of the IV international conference on forest fire research. 18–23 Nov 2002, Luso, Coimbra, Portugal*. Millpress Scientific Publications, Rotterdam, pp 1–10
- Cumming S (2001) A parametric model of the fire-size distribution. *Can J For Res* 31:1297–1303
- Dawes WR, Short D (1994) The significance of topology for modeling the surface hydrology of fluvial landscapes. *Water Resour Res* 30:1045–1055
- De Vasconcelos MP, Silva S, Tome M, Alvim M, Pereira JC (2001) Spatial prediction of fire ignition probabilities: comparing logistic regression and neural networks. *Photogramm Eng Remote Sens* 67:73–81
- DeFries R, Pandey D (2010) Urbanization, the energy ladder and forest transitions in India's emerging economy. *Land Use Policy* 27:130–138
- Demir M (2007) Impacts, management and functional planning criterion of forest road network system in Turkey. *Transp Res Part A Policy Pract* 41:56–68
- Devi LM, Bandooni S, Prasad AS (2015) The use of remote sensing and GIS for Managing forest plantation and watershed conservation in Pasolgad watershed in Pauri Garhwal, Uttarakhand. *TTPP*, vol 1, p 465
- Dimri P, Gunwant H (2012) Conceptual model for developing meteorological data warehouse in Uttarakhand-a review. *J Inf Oper Manag* 3:107
- Dobhal GL (2005) Development of the hill areas: a case study of pauri garhwal district. Concept Publishing Company, Delhi
- Dong X, Li-min D, Guo-fan S, Lei T, Hui W (2005) Forest fire risk zone mapping from satellite images and GIS for Baihe Forestry Bureau, Jilin China. *J For Res* 16:169–174
- Elavarasan V, Gusain V, Das T, Pal A, Kumar S, Hasan S, Jain H, Biswas T, Singh N (2019) Experiences from nation-wide adoption of satellite based near real time forest fire alerts to improve forest fire management in India. *Biodivers Bras* 1:197

- Erten E, Kurgun V, Musaoglu N (2004) Forest fire risk zone mapping from satellite imagery and GIS: a case study. In: XXth international society for photogrammetry and remote sensing congress, Istanbul, Turkey, 12–23 July 2004
- Eskandari S (2017) A new approach for forest fire risk modeling using fuzzy AHP and GIS in Hyrcanian forests of Iran. *Arab J Geosci* 10:190
- Eugenio FC, dos Santos AR, Fiedler NC, Ribeiro GA, da Silva AG, dos Santos ÁB, Paneto GG, Schettino VR (2016) Applying GIS to develop a model for forest fire risk: a case study in Espírito Santo Brazil. *J Environ Manag* 173:65–71
- Falkowski MJ, Gessler PE, Morgan P, Hudak AT, Smith AM (2005) Characterizing and mapping forest fire fuels using ASTER imagery and gradient modeling. *For Ecol Manag* 217:129–146
- Fao I, WFP (2015) The state of food insecurity in the world, pp 1–62
- Finney MA (1998) FARSITE, Fire area simulator--model development and evaluation; US department of agriculture, forest service, Rocky mountain research station
- Flannigan M, Wotton B, Marshall G, De Groot W, Johnston J, Jurko N, Cantin A (2016) Fuel moisture sensitivity to temperature and precipitation: climate change implications. *Clim Change* 134:59–71
- Fornacca D, Ren G, Xiao W (2018) Evaluating the best spectral indices for the detection of burn scars at several post-fire dates in a mountainous region of Northwest Yunnan China. *Remote Sens* 10:1196
- Frandsen WH (1971) Fire spread through porous fuels from the conservation of energy. *Combust Flame* 16:9–16
- FSI (2019) India state of forest report 2019. Forest survey of India, Ministry of Environment and Forest, Dehradun, vol 1. <http://fsi.nic.in/forest-report-2019>
- Gairola S, Sharma C, Ghildiyal S, Suyal S (2012) Chemical properties of soils in relation to forest composition in moist temperate valley slopes of Garhwal Himalaya India. *Environ* 32:512–523
- Gaither CJ, Poudyal NC, Goodrick S, Bowker J, Malone S, Gan J (2011) Wildland fire risk and social vulnerability in the Southeastern United States: an exploratory spatial data analysis approach. *For Policy Econ* 13:24–36
- Gamon JA, Field CB, Goulden ML, Griffin KL, Hartley AE, Joel G, Peñuelas J, Valentini R (1995) Relationships between NDVI, canopy structure, and photosynthesis in three Californian vegetation types. *Ecol Appl* 5:28–41
- Gandhi GM, Parthiban S, Thummalu N, Christy A (2015) NDVI: vegetation change detection using remote sensing and GIS—A case study of Vellore district. *Proc Comput Sci* 57:1199–1210
- Gardner RH, Romme WH, Turner MG (1999) Predicting forest fire effects at landscape scales. Spatial modeling of forest landscape change: approaches and applications. Cambridge University Press, Cambridge, pp 163–185
- Gaur RD, Bartwal BS (1993) Different types of forest communities in Pauri District (Garhwal Himalaya). In: Rajwar GS (ed) Garhwal Himalaya: ecology and environment, vol 1. Ashish Publishing House, New Delhi, pp 131–147
- Greco S, Figueira J, Ehrigott M (2016) Multiple criteria decision analysis. Springer, Berlin
- Guarnieri F, Andersen CK, Olampi S, Chambinaud N (1998) FireLab, towards a problem solving environment to support forest fire behaviour modelling. In: Viegas DX (ed) Proceedings of the third international conference on forest fire research, vol 2718. University of Coimbra, Coimbra, Portugal, pp 483
- Hargrove WW, Gardner R, Turner M, Romme W, Despain D (2000) Simulating fire patterns in heterogeneous landscapes. *Ecol Model* 135:243–263
- Hashjin SS, Milaghardan AH, Esmaeily A, Mojaradi B, Naseri F (2012) Forest fire hazard modeling using hybrid AHP and fuzzy AHP methods using MODIS sensor. In: Proceedings of 2012 IEEE international geoscience and remote sensing symposium; pp 931–934
- Hayes GL (1941) Influence of altitude and aspect on daily variations in factors of forest-fire danger, US department of agriculture
- Heinsch FA, Andrews PL (2010) BehavePlus fire modeling system, version 5.0: design and features. General technical reports RMRS-GTR-249. Fort Collins, CO: US Department of agriculture, forest service, rocky mountain research station, 111 p 249.
- Hilton J, Sullivan AL, Swedosh W, Sharples J, Thomas C (2018) Incorporating convective feedback in wild-fire simulations using pyrogenic potential. *Environ Model Softw* 107:12–24
- Hong H, Chen W, Xu C, Youssef AM, Pradhan B, Tien Bui D (2017) Rainfall-induced landslide susceptibility assessment at the Chongren area (China) using frequency ratio, certainty factor, and index of entropy. *Geocarto Int* 32:139–154
- Hosonuma N, Herold M, De Sy V, De Fries RS, Brockhaus M, Verchot L, Angelsen A, Romijn E (2012) An assessment of deforestation and forest degradation drivers in developing countries. *Environ Res Lett* 7:044009
- Hughes AC (2018) Have Indo-Malaysian forests reached the end of the road? *Biol Cons* 223:129–137

- Iwan R, Limberg G, Moeliono M, Sudana M, Wollenberg E (2004) Mobilizing community conservation. A community initiative to protect its forest against logging in Indonesia. In: Paper prepared for the panel 'Nontrivial pursuits: logging, profits and politics in local forest practices in Indonesia', at the 10th Biennial Conference of the International Association for the Study of Common Property (IASCP), Oaxaca, Mexico, 9–13 Aug 2004
- Jadhav A, Saini P, Ravindra A, Singh S (2019) Increasing forest or forest cover in India. *Curr Sci* 116:158
- Jain A, Ravan SA, Singh R, Das K, Roy P (1996) Forest fire risk modeling using remote sensing and geographic information system. *Curr Sci* 70:928–933
- Jain S, Kumar V, Saharia M (2013) Analysis of rainfall and temperature trends in northeast India. *Int J Climatol* 33:968–978
- Jaiswal RK, Mukherjee S, Raju KD, Saxena R (2002) Forest fire risk zone mapping from satellite imagery and GIS. *Int J Appl Earth Obs Geoinf* 4:1–10
- Jazireie M (2005) Forest maintenance. Publishing and Printing Institute of Tehran University, Tehran, Iran
- Jiang H, Eastman JR (2000) Application of fuzzy measures in multi-criteria evaluation in GIS. *Int J Geogr Inf Sci* 14:173–184
- Kahraman C, Cebeci U, Ulukan Z (2003) Multi-criteria supplier selection using fuzzy AHP. *Logist Inform Manag* 16:382–394
- Kanga S, Tripathi G, Singh SK (2017) Forest fire hazards vulnerability and risk assessment in Bhajji forest range of Himachal Pradesh (India): a geospatial approach. *J Remote Sens GIS* 8:1–16
- Karafyllidis I, Thanailakis A (1997) A model for predicting forest fire spreading using cellular automata. *Ecol Model* 99:87–97
- Kayet N, Chakrabarty A, Pathak K, Sahoo S, Dutta T, Hatai BK (2018) Comparative analysis of multi-criteria probabilistic FR and AHP models for forest fire risk (FFR) mapping in Melghat tiger reserve (MTR) forest. *J For Res* 31:1–15
- Keane RE, Burgan R, van Wagtenonk J (2001) Mapping wildland fuels for fire management across multiple scales: integrating remote sensing, GIS, and biophysical modeling. *Int J Wildland Fire* 10:301–319
- Kumari S, Mehta J, Shafi S, Dhiman P (2017) Phytosociological analysis of woody vegetation under burnt and unburnt oak dominated forest at Pauri, Garhwal Himalaya India. *Environ Conserv J* 18:99–106
- Liu S, Yang J (2013) Modeling spatial patterns of forest fire in Heilongjiang Province using generalized linear model and maximum entropy model. *Chin J Ecol* 32:1620–1628
- Ljubomir G, Pamućar D, Drobnjak S, Pourghasemi HR (2019) Modeling the spatial variability of forest fire susceptibility using geographical information systems and the analytical hierarchy process. *Spatial modeling in GIS and R for earth and environmental sciences*. Elsevier, Amsterdam, pp 337–369
- Mahdavi A (2012) Forests and rangelands? wildfire risk zoning using GIS and AHP techniques. *Casp J Environ Sci* 10:43–52
- Mallick J, Khan RA, Ahmed M, Alqadhi SD, Alsuhbi M, Falqi I, Hasan MA (2019) Modeling Ground-water potential zone in a semi-arid region of Aseer using Fuzzy-AHP and geoinformation techniques. *Water* 11:2656
- Mermoz M, Kitzberger T, Veblen TT (2005) Landscape influences on occurrence and spread of wildfires in Patagonian forests and shrublands. *Ecology* 86:2705–2715
- Meten M, Bhandary NP, Yatabe R (2015) GIS-based frequency ratio and logistic regression modeling for landslide susceptibility mapping of Debre Sina area in central Ethiopia. *J Mt Sci* 12:1355–1372
- Mohammadi F, Bavaghar MP, Shabani N (2014) Forest fire risk zone modeling using logistic regression and GIS: an Iranian case study. *Small scale For* 13:117–125
- Mondal N, Sukumar R (2016) Fires in seasonally dry tropical forest: testing the varying constraints hypothesis across a regional rainfall gradient. *PLoS ONE* 11:e0159691
- Negi M, Kumar A (2016) Assessment of increasing threat of forest fires in Uttarakhand, using remote sensing and GIS techniques. *Glob J Adv Res* 3:457–468
- Negnevitsky M (2005) Artificial intelligence: a guide to intelligent systems. Pearson education, London
- Noble I, Gill A, Bary G (1980) McArthur's fire-danger meters expressed as equations. *Aust J Ecol* 5:201–203
- Nuthammachot N, Stratoulas D (2019) A GIS-and AHP-based approach to map fire risk: a case study of Kuan Kreng peat swamp forest, Thailand. *Geocarto Int*. <https://doi.org/10.1080/10106049.2019.1611946>
- Oliveira S, Oehler F, San-Miguel-Ayanz J, Camia A, Pereira JM (2012) Modeling spatial patterns of fire occurrence in Mediterranean Europe using multiple regression and random forest. *For Ecol Manag* 275:117–129
- Pandey K, Ghosh S (2018) Modeling of parameters for forest fire risk zone mapping. *ISPRS Int Arch Photogramm, Remote Sens Spatial Inf Sci*, XLII 5:299–304

- Park S, Jeon S, Kim S, Choi C (2011) Prediction and comparison of urban growth by land suitability index mapping using GIS and RS in South Korea. *Landscape Urban Plan* 99:104–114
- Petropoulos G, Knorr W, Scholze M, Boschetti L, Karantounias G (2010) Combining ASTER multispectral imagery analysis and support vector machines for rapid and cost-effective post-fire assessment: a case study from the Greek wildland fires of 2007. *Nat Hazards Earth Syst Sci* 10:305–317
- Pettorelli N, Vik JO, Mysterud A, Gaillard J-M, Tucker CJ, Stenseth NC (2005) Using the satellite-derived NDVI to assess ecological responses to environmental change. *Trends Ecol Evol* 20:503–510
- Porwal M, Meir M, Hussin Y, Roy P, Spatial modeling for fire risk zonation using remote sensing and GIS. In: Proceedings of ISPRS commission VII working group II workshop on application of remote sensing and GIS for sustainable development, Hyderabad
- Pourghasemi HR (2016) GIS-based forest fire susceptibility mapping in Iran: a comparison between evidential belief function and binary logistic regression models. *Scand J For Res* 31:80–98
- Pourghasemi HR, Beheshtirad M, Pradhan B (2016) A comparative assessment of prediction capabilities of modified analytical hierarchy process (M-AHP) and Mamdani fuzzy logic models using Netcad-GIS for forest fire susceptibility mapping. *Geom Nat Hazards Risk* 7:861–885
- Pourtaghi ZS, Pourghasemi HR, Rossi M (2015) Forest fire susceptibility mapping in the Minudasht forests, Golestan province Iran. *Environ Earth Sci* 73:1515–1533
- Pradhan B, Suliman MDHB, Awang MAB (2007) Forest fire susceptibility and risk mapping using remote sensing and geographical information systems (GIS). *Disaster Prev Manag Int J* 16:344–352
- Rahmati O, Pourghasemi HR, Zeinivand H (2016) Flood susceptibility mapping using frequency ratio and weights-of-evidence models in the Golestan Province Iran. *Geocarto Int* 31:42–70
- Rawat GS (2003) Fire Risk Assessment for forest fire control management in Chilla forest range of Rajaji National Park Uttarakhand (India). MSc Thesis, International Institute for Geoinformation Science and Earth Observation Enschede of the Netherlands, 74 pp
- Ruelland D, Ardoin-Bardin S, Billen G, Servat E (2008) Sensitivity of a lumped and semi-distributed hydrological model to several methods of rainfall interpolation on a large basin in West Africa. *J Hydrol* 361:96–117
- Saaty TL (1980) The analytic hierarchy process, planning, priority setting, resource allocation. McGraw-Hill, London
- Sahana M, Ganaie TA (2017) GIS-based landscape vulnerability assessment to forest fire susceptibility of Rudrapur district, Uttarakhand India. *Environ Earth Sci* 76:676
- Sahoo S, Munusamy SB, Dhar A, Kar A, Ram P (2017) Appraising the accuracy of multi-class frequency ratio and weights of evidence method for delineation of regional groundwater potential zones in canal command system. *Water Resour Manag* 31:4399–4413
- Saklani P (2008) Forest fire risk zonation, A case study Pauri Garhwal, Uttarakhand, India. MSc thesis, International Institute for Geo-information Science and Earth Observation Enschede of the Netherlands and Indian Institute of Remote Sensing (NRSA), Dehradun, India, 71 pp
- Satir O, Berberoglu S, Donmez C (2016) Mapping regional forest fire probability using artificial neural network model in a Mediterranean forest ecosystem. *Geom Nat Hazards Risk* 7:1645–1658
- Schillaci C, Braun A, Kropáček J (2015) Terrain analysis and landform recognition. *Geomorphol Tech* 2:1–18
- Senici D, Chen HY, Bergeron Y, Cyr D (2010) Spatiotemporal variations of fire frequency in central boreal forest. *Ecosystems* 13:1227–1238
- Shahabi H, Hashim M, Ahmad BB (2015) Remote sensing and GIS-based landslide susceptibility mapping using frequency ratio, logistic regression, and fuzzy logic methods at the central Zab basin Iran. *Environ Earth Sci* 73:8647–8668
- Sharma N, Hussin YA (1996) Spatial modeling for forest fire hazard prediction, management and control in Corbett national park, India. In: Saramaki J, Koch B, Lund HG (eds) Remote sensing and computer technology for natural resources assessment. Proceedings of the subject group S4. 02-00. Forest resource inventory and monitoring and subject group S4. 12-00 Remote Sensing Technology, vol II. IUFRO XX World congress, 6–12 Aug 1995, Tampere, Finland. University of Joensuu, Faculty of Forestry, pp 185–192
- Sharma CM, Baduni NP, Gairola S, Ghildiyal SK, Suyal S (2010) Tree diversity and carbon stocks of some major forest types of Garhwal Himalaya India. *For Ecol Manag* 260:2170–2179
- Sharma LK, Kanga S, Nathawat MS, Sinha S, Pandey PC (2012) Fuzzy AHP for forest fire risk modeling. *Disaster Prev Manag Int J* 21(2):160–171. <https://doi.org/10.1108/09653561211219964>
- Sörensen R, Zinko U, Seibert J (2006) On the calculation of the topographic wetness index: evaluation of different methods based on field observations. *Hydrol Earth Syst Sci* 10:101–112
- Stipaničev D, Vuko T, Bodrožić L, (2007) Location determination of automatic forest fire monitoring stations based on AHP and GIS data. In: Proceedings of TIEMS (The International Emergency Management Society) 2007 international conference
- Suryabhagavan K, Alemu M, Balakrishnan M (2016) GIS-based multi-criteria decision analysis for forest fire susceptibility mapping: a case study in Harena forest, southwestern Ethiopia. *Trop Ecol* 57:33–43



- Tarboton DG (1997) A new method for the determination of flow directions and upslope areas in grid digital elevation models. *Water Resour Res* 33:309–319
- Taylor SW, Alexander ME (1996) Field guide to the Canadian forest fire behavior prediction (FBP) system. (BINDER), vol 11
- Thakur AK, Singh D (2014) Forest fire risk zonation using geospatial techniques and analytic hierarchy process in Dehradun district, Uttarakhand, India. *Univ J Environ Res Technol* 4:82–89
- Tiryaki F, Ahlatcioglu B (2009) Fuzzy portfolio selection using fuzzy analytic hierarchy process. *Inf Sci* 179:53–69
- Torres FTP, Romeiro JMN, de Albuquerque Santos AC, de Oliveira Neto RR, Lima GS, Zanuncio JC (2018) Fire danger index efficiency as a function of fuel moisture and fire behavior. *Sci Total Environ* 631:1304–1310
- Troeh FR (1965) Landform equations fitted to contour maps. *Am J Sci* 263:616–627
- Tyagi B, Veer V (2016) Entomology in the Doon Valley (Garhwal Himalaya) a stronghold for insect research. Scientific Publishers, Jodhpur
- Vahidnia M, Alesheikh A, Alimohammadi A, Bassiri A (2008) Fuzzy analytical hierarchy process in GIS application. *Int Arch Photogramm Remote Sens Spatial Inf Sci* 37:593–596
- Vakalis D, Sarimveis H, Kiranoudis C, Alexandridis A, Bafas G (2004) A GIS based operational system for wildland fire crisis management I. Mathematical modeling and simulation. *Appl Math Model* 28:389–410
- Van der Werf GR, Randerson JT, Giglio L, Collatz G, Mu M, Kasibhatla PS, Morton DC, DeFries R, Jin Y, van Leeuwen TT (2010) Global fire emissions and the contribution of deforestation, savanna, forest, agricultural, and peat fires (1997–2009). *Atmos Chem Phys* 10:11707–11735
- van Wagner CE (1967) Calculations on forest fire spread by flame radiation. Canadian Department of Forestry and Rural Development, Forestry Branch Departmental Publication, vol 24717, p 18
- Vega JA, Cuiñas P, Fonturbel T, Pérez-Gorostiaga P, Fernandez C (1998) Predicting fire behaviour in Galician (NW Spain) shrubland fuel complexes. In: Viegas DX (ed) Proceedings of the third international conference on forest fire research. University of Coimbra, Luso, Portugal, pp 713–728
- Viegas DX (2004) Slope and wind effects on fire propagation. *Int J Wildland Fire* 13:143–156
- Wallace L (1946) Analysis of fire spread in light forest fuels. *J Agric Res* 72:93
- Wang Y-M, Luo Y, Hua Z (2008) On the extent analysis method for fuzzy AHP and its applications. *Eur J Oper Res* 186:735–747
- Wang L, Hunt ER Jr, Qu JJ, Hao X, Daughtry CS (2013) Remote sensing of fuel moisture content from ratios of narrow-band vegetation water and dry-matter indices. *Remote Sens Environ* 129:103–110
- Weber R (1989) Analytical models for fire spread due to radiation. *Combust Flame* 78:398–408
- Wood LJ, Dragicevic S (2007) GIS-based multicriteria evaluation and fuzzy sets to identify priority sites for marine protection. *Biodivers Conserv* 16:2539–2558
- Wu Z, Zhang H, Krause CM, Cobb NS (2010) Climate change and human activities: a case study in Xinjiang China. *Clim Change* 99:457–472
- Yebrá M, Dennison PE, Chuvieco E, Riano D, Zylstra P, Hunt ER Jr, Danson FM, Qi Y, Jurdao S (2013) A global review of remote sensing of live fuel moisture content for fire danger assessment: moving towards operational products. *Remote Sens Environ* 136:455–468
- Zadeh LA (1965) Fuzzy sets. *Inf Control* 8:338–353
- Zammit O, Descombes X, Zerubia J (2006) Burnt area mapping using support vector machines. *For Ecol Manag* 234:S240
- Zhang D, Han S, Zhao J, Zhang Z, Qu C, Ke Y, Chen X (2009) Image based forest fire detection using dynamic characteristics with artificial neural networks. In: Proceedings of 2009 international joint conference on artificial intelligence, pp 290–293
- Zhang Q, Xu J, Xu L, Guo H (2016) Deep convolutional neural networks for forest fire detection. In: Proceedings of 2016 international forum on management, education and information technology application
- Zimmermann HJ (2010) Fuzzy set theory. *Wiley Interdisciplinary Reviews: Computational Statistics* 2:317–332

## Affiliations

Anuj Tiwari<sup>1</sup>  · Mohammad Shoab<sup>2</sup> · Abhilasha Dixit<sup>3</sup>

Mohammad Shoab  
mshoab@su.edu.sa

Abhilasha Dixit  
adixit@dm.iitr.ac.in

<sup>1</sup> Department of Civil Engineering, Indian Institute of Technology, Roorkee, Uttarakhand, India

<sup>2</sup> Department of Computer Science, College of Science and Humanities, Shaqra University, Al Dawadmi, Riyadh Province, Kingdom of Saudi Arabia

<sup>3</sup> Centre of Excellence in Disaster Mitigation and Management, Indian Institute of Technology, Roorkee, Uttarakhand, India